STUDIES OF CLUMP STRUCTURE OF PHOTODISSOCIATION REGIONS AT MILLIMETER AND SUB-MILLIMETER WAVELENGTHS

DISSERTATION
SUBMITTED FOR THE DEGREE OF
Master of Philosophy
IN
PHYSICS

BY
SYED SALMAN ALI

DEPARTMENT OF PHYSICS
ALIGARH MUSLIM UNIVERSITY
ALIGARH (INDIA)
1994

IN LOVING MEMORY OF

MY MOTHER

DEPARTMENT OF PHYSICS
ALIGARH MUSLIM UNIVERSITY
ALIGARH—202 002 (India)
Phone: 2 9 0 0 1
Telex : 564—230 AMU IN

CERTIFICATE

Certified that the work presented in this dissertation is the original work of **MR. SYED SALMAN ALI** done under my supervision.

(ABDUL QAIYUM)
Reader

ACKNOWLEDGEMENT

I avail this opportunity to express my heart-felt gratitude to my research supervisor **Dr. Abdul Qaiyum**, Reader Deptt. of Physics, A.M.U. Aligarh, who introduced me to the subject and has been a constant source of inspiration and motivation throughout the present study. It is only due to his valuable suggestions, spirited guidance and enthusiastic supervision that this work has been completed.

I am also thankful to **Prof. M.S.Z. Chaghtai**, Chairman Deptt. of Physics, A.M.U. Aligarh, for allowing me to carryout the present study and very kindly extending every facility available in the department.

My sincere thanks are also due to **Prof. S.M.R. Ansari** and **Mr. Badre Alam**, lecturer, Deptt. of Physics, A.M.U. Aligarh, for their affection, cooperation and encouragement throughout the present endeavour.

I am also indebted to my colleagues and the non teaching staff of the deptt. of Physics, A.M.U. Aligarh, for their cooperation and help whenever it was needed.

It will be a serious lapse if I fail to acknowledge the moral support of my family members as they encouraged and motivated me to keep it up time and again.

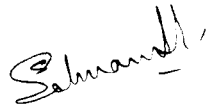

(Syed Salman Ali)

TABLE OF CONTENTS

CHAPTER - 1

INTRODUCTION

CHAPTER - 1

INTRODUCTION

The molecular clouds are ionized by the intense FUV (far ultra violet) radiation producing HII region if the cloud finds itself in the proximity of an intense ionizing source, i.e. O and B stars providing an FUV flux 10^3- 10^6 times more intense than the average ambient interstellar field. On the interface of molecular clouds and HII region there is a region commonly known as Photodissociation Region (PDR). Some times this is also called CII region. The basic models of PDRs generally include a hot (100-1000K) layer of atomic gas (H, C^+, O) a warm (150-100K) partially dissociated region in which atomic hydrogen and ionized carbon are transformed into H_2 and C or CO respectively and a deep cooler ($T<100K$) region in which oxygen is found to be in atomic form as a result of photodissociation. But with a reduced abundance. Apart from the PDRs which seperate the HII regions from their parental molecular clouds these models are also applicable to the neutral shell around the planetary nebulae, bright rimmed clouds, reflection nebulae and the regions surrounding the protostars. The depth of PDR's is funtion of FUV radiation, density and attenuation parameters of the gas. During the last decade detailed studies of PDRs (CII regions) have been made by Bennet et al.(1993); Castets et.al.(1990); Howe et

al. (1991); Meixner and Tielens et al.(1993); Sciama (1993); Stutzki (1988); Robert and Pagani (1993); Turbur and Goldsmith (1993); Tielens and Hollenbach (1985 a,b) and Wolfire et.al. (1989,890)

Generally to study the individual PDRs models of Tielens and Hollenbach (1985a) {here after TH} are employed. These models are developed on the detailed formulation of gas chemistry, thermal balance and radiative transfer of the cooling lines in the atomic and molecular components. The dense gas is illuminated by the FUV ($6eV<h\nu<13.6eV$) flux $Go=10^{3} - 10^{6}$, where Go is the FUV field expressed in units of local Galictic FUV flux (1.6×10^{-3}ergs cm^{-2} s^{-1} in units of one dimensional flux or 1.3×10^{-4} ergs cm^{-2} $s^{-1}sr^{-1}$ in units of intensity ; Habing 1968) which is characterised by a sharp cut off at the Lyman limits ($h\nu$ = 13.6 eV). The Lyman continuum photons are supposed to be absorbed in HII regions which lie outside the PDR or adjacent to it. The dust grains absorbs the incident FUV radiation and radiates in the infrared continuum .

The gas in the proximity of HII region is heated via the photoelectric ejection of electrons from the grains. In this region gas consists of atomic species i.e. HI, HeI, NI, OI and singly ionized species i.e. CII, SiII, FeII and other heavy elements having ionization potential less than 13.6 eV and cools mainly in the OI (63μm and 145μm), CII (158μm) and

Si II (35μm) fine structure lines. In some cases other fine structure transitions too play an important role as far as cooling is concerned. At larger optical depths the gas is mostly molecular i.e. H_2, CO but atomic oxygen prevails even in the deep molecular gas provided temperature is not too low. If FUV flux is small then CI (609 & 370) lines become important coolant close to the boundary of HII regions. The gas is still heated by the photo elctrons but the prime coolants are the rotational lines of CO . If we go furthur inside, the other heating processes start to compete with the grain heating mechanism .

The one dimensional models proposed by TH (1985a) are good enough to provide the solution for the gas phase atomic and molecular compositions, the energy balance and the radiative transfer of cooling lines. But one component models of TH assume that the region is homogeneous and line radiation escapes only through one face of the cloud because in this model escape probabilty formulation of de Jong et.al. (1980) has been employed, in which cloud is assumed to be semi-infinite. This assumption is contrary to the observational studies. Observationally it has been found that large number of infra-red and millimeter observations are optically thin.

However, models have been proved succesful in reproducing the several cooling line intensities but they

fail to manifest many of the observed features. Most notably the scale size of the PDR line emission, which is observed to be many order of magnitude larger than that predicted by the homogeneous models (e.g. Stutzki et.al.1988; Howe et.al.1991) besides this the very strong emission lines (CO J =14-13) are found to be anomalously stronger than that predicted by the uniform density and temperature regions. For example, the SiII (35μm) line intensity has been observed to be significantly stronger than the OI (63μm) line intensity in many of these regions. These models are also unable to account for the extended CII emission which extends over several parsecs throughout the molecular cloud, likewise the CO (J = 14-13) and OI (145μm) spectra indicate high temperature (2000 - 4000K) and densities (a few 10^4 cm^{-3}) for both molecular and atomic gas in the interface as compared to the homogeneous density models.

The analysis of the observed data together with the earlier observations of molecular and ionized gas suggests that by taking the homogeneous desity distribution the models yield densities and temperatures of the order of 3 x 10^4 cm^{-3} and 300K respectively, for Orion complex. As discussed above the homogeneous models fail on several accounts to reproduce the obsevred spatial distribution, intensities and line ratios. Several authors have proposed the three component models (Stutzki et.al. 1988; Meixner et.al. 1992; and

Meixner and Tielens 1993) in which PDRs consists of clumps having density ~ $10^{9} cm^{-3}$. This clumpy core is surrounded by a halo with density 300 cm^{-3}. These models agree well with the observed spatial distributions and sub-millimeter line emission.

According to the three component models the SiII (35μm) line emission as compared to OI (63μm) line can be attributed to the high column density of clumps and the self absorption of OI (63μm) line in the interclump medium if the PDR is seen edge on. The OI, SiII, and high J CO line emission originate in the dense clumps, whereas the CII, CI, and low - J CO line emission is characterised by the interclump medium and the extended CII and CI emission confirms the presence of halo.

The homogeneous models of TH calculate the temperature structure and line intensities of different atomic, ionic and molecular species with the assumption that the regions facing the observer are irradiated by large UV fluxes and lines can escape only towards the observer and hence the medium is behaving like a semi-infinite atmosphere (de Jong et. al.1980). But the observational studies show that most of the FIR and sub millimeter line emission of atoms and molecules are optically thin except OI (63μm) and few low rotational transitions of CO and other molecules. These observations are contrary to the optically thick (semi-infinite slab) assumption of de Jong et. al. (1980).

In the present study an attempt has been made to incorporate the escape of photons from both sides of the region. For this purpose it is supposed that the cloud is a finite plane parallel slab. The radiative transfer is solved in one dimensional approach and techniques of Averett and Hummer (1965) have been used. Here density is taken as a free parameter and for turbulent velocity and flux observationally derived values are used. Here we are more interested in the study of the validity of TH model for a range of parameters. Since the nature of the study is purely investigative, therefore, no attempt has been made to study the variety of PDRs. However, the present formulation has been employed to study the region of M17 assuming it as filled with clumps instead of being homogeneous.

The calculations show that most of the lines are originating from the clumps. Theoretically extended line emission are possible in the case of CII (158μm), CI (307, and 609μm), OI (63μm) and CO (1-0) emissions. Observationally the lines from CII and CI are found from extended region. The agreement of calculated values and that of the observations over a wide range of fine structure line emissions and rotational transitions favour clumpiness in the region and the densities are ~ 6×10^5 and 4×10^3 for the clump and interclump region respectively. Also higher rotational transitions of CO molecules which are optically

thin are modified by an order of magnitude if photons are cosiderd to escape from both sides of slab. In such cases the use of present formalism may have consequential effects in the interpretation of lines. At high density far greater than the critical where radiative processes have no role to play the TH model can be employed safely.

CHAPTER - 2

MODEL FOR PHOTODISSOCIATION REGIONS

CHAPTER - 2

MODEL FOR PHOTODISSOCIATION REGIONS

Photodissociaton regions are studied through the FIR and sub millimeter line emission of CI (307 & 608μm), CII (158μm), OI (63 & 145μm), SiII (35μm), FeII (26μm) and rotational transitions of CO (ΔJ = 1 to = 20). To study the physical properties of the photodissociation regions Tielens and Hollenbach have developed theoretical models. Basically these theoretical models attempts to calculate the temperature structure of the region and line intensities of the fine structure transitions of atoms and ions and rotational transitions of molecuels. In TH models the emitting region is supposed to be semi-infinite slab. As a result only half of the photons are able to escape from the cloud and those photons which are emitted from the semi-infinite slab do not escape.

Recent observational studies of FIR and sub millimeter transitions show that most of these lines are optically thin except OI (63μm) and few low lying rotational transitions of CO. In the light of these observational facts the optically thick (semi-infinite slab) assumption of de Jong et.al. (1980), extensively used in TH models to calculate the escape probability is not a safe approximation.

2.1 Escape of Radiation Through PDR:

In order to meet these observational facts the escape probability formalism should include the escape of photons from both sides of the slab. For this purpose the radiative transfer equation in a plane parallel slab and isotropic source for distance z and normal to the plane can be written as,

$$\mu \, dI_\nu/d\tau_\nu = \phi_\nu (x) [I_\nu(\tau_\nu, \mu) - S_\nu(\tau_\nu)] \quad \text{---------- (2.1)}$$

The solution of the transfer equation depends upon the boundary conditions. Two problems of fundamental importance in Astrophysics are those of a finite slab of material, or of a medium (e.g.stellar atmosphere) that has a boundary on one side but is so thick on the other side that it can be imagined to as extending to infinity-the semi infinite atmosphere.

For the finite slab problem we may specify a total geometrical thickness z and a total optical thickness T_ν, following the convention, the optical depth is taken to run from 0 to T_ν, away from the observer while the geometrical depth scale runs from 0 to z towards the observer. ϕ_ν is the line profile at frequency ν. To obtain a unique solution of the transfer equation, we must specify the incident radiation field on both faces of the slab. Measuring θ to be positive away from the observer, $\mu = \cos\theta$ will be greater than zero for pencils of radiation moving towards the observer and less

than zero for pencils moving away. Thus we specify the boundary functions f and g such that,

$$I_\nu (0,\mu) = f_\nu (\mu)$$

---------- (2.2)

for $-1 \leq \mu \leq 0$ at the upper boundary, and for $0 \leq \mu \leq 1$,

$$I_\nu (T_\nu,\mu) = g_\nu (\mu)$$

---------- (2.3)

for the lower boundary. Given these boundary conditions and a complete specification of sources and sinks of energy within the slab, the radiation field follows directly from the solution of the transfer equation (2.1)

In the semi infinite case we need to specify only the radiation field incident upon the upper boundary i.e. equation (2.2). Since there is no lower boundary in the semi infinite case, therefore, equation (2.3) is not applicable but is replaced by boundedness requirement. Specifically, we demand that at great depths the radiation field should satisfy the relation,

$$\lim_{\tau_\nu \to \infty} I_\nu (\tau_\nu ,\mu) \exp (-\tau_\nu/\mu) = 0$$

---------- (2.4)

Before writnig the formal solution of the equation of transfer, it is instructive to consider a few simple examples

(a) Suppose no material is present. Then k_ν (absorption coefficient) and j_ν (emission coefficient) both are zero. Thus I_ν is constant. This result is consistent with the well

known principle of the invariance of specific intensity when no sources or sinks are present.

(b) Suppose that emitting material is present but there is no opacity at the frequency under consideraion. then,

$$\mu \, dI_\nu / d\tau_\nu = J_\nu \qquad \text{---------- (2.5)}$$

and for a finite slab emergent intensity is given by the expression,

$$I_\nu (0,\mu) = 1/\mu \int_0^z J_\nu(z) \, dz + I_\nu (T,z) \qquad \text{---------- (2.6)}$$

This expression is of interest physically in the formation of optically forbidden lines in nebulae. In such lines atoms are excited to metastable levels by collisions, and subsequently some of these decay and emit photon. The absorption probability for such a forbidden transition is negligible compared to other processes that are depopulating the lower level. Thus, in effect, photons are created at the expense of the thermal energy pool of the gas, but none are destroyed by absorption. This situation, incidentally is far from LTE.

(c) Suppose that there is absorption of radiation in the medium but no emission , then,

$$dI_\nu = - k_\nu I_\nu \, dz/\mu \qquad \text{---------- (2.7)}$$

and again for a finite slab the emergent radiation is given by the expression,

$$I_\nu(0,\mu) = I_\nu(T_\nu,\mu)\exp(-1/\mu\int_o^z k_\nu\,dz)$$
$$= I_\nu(T_\nu,\mu)\exp(-T_\nu/\mu)$$
---------- (2.8)

Equation (2.8) is of relevance physically when photons absorbed in the material are converted into photons of another frequency before being reemitted or are destroyed and converted directly to the kinetic energy of the particles in the absorbing medium.

Mathematically the equation of radiatve transafer eq (2.1) is a linear first order differential equation with constant coefficients. Its general solution will contain all the ingredients discussed above.The equation can be solved in the following way. Supressing the subscript in equation (2.1) for convenience, we have,

$$\mu\, dI/d\tau = \phi(I - S)$$ ---------- (2.9)

or $$\mu\, dI/d\tau = \phi I - \phi S$$ ---------- (2.10)

The above differential equation must have an integrating factor, namely $\exp(-\tau/\mu)$, thus,

$$d/d\tau\,[I\exp(-\tau\phi/\mu)] = -S\exp(-\tau\phi)/\mu$$
---------- (2.11)

So that,

$$|_{\tau_1}^{\tau_2} I\exp(-\tau\phi/\mu) = -\int_{\tau_1}^{\tau_2} S(t)\exp(-t\phi/\mu)\phi\,dt/\mu$$
---------- (2.12)

or $$I(\tau_1,\mu) = I(\tau_2,\mu)\, e^{-\{(\tau_1-\tau_2)\phi/\mu\}}$$
$$+\int_{\tau_1}^{\tau_2} S(t)\, e^{-\{(t-\tau_1)\phi/\mu\}}\phi/\mu\,dt$$ ---------- (2.13)

For example suppose we set $\tau_1 = 0$ and take the limit as $\tau_2 \to \infty$;thus we compute the emergent intensity of a semi -infinite atmosphere. Then by virtue of equation (2.4)

$$I(0,\mu) = \int_0^\infty S(t)\, e^{-t\phi/\mu}\, \phi/\mu\, dt \qquad \text{---------- (2.14)}$$

Physically this merely states that the emergent intensity is given by a weighted mean over the source function - The weighting factor corresponds to the surface from each element of optical depth.

As second example, consider a finite slab of thickness T, within which S is constant and upon which there is no incident radiation. Then the normally emergent radiation is,

$$I = S\,(1 - e^{-T}) \qquad \text{---------- (2.15)}$$

For $T \gg 1$, $I = S$. This is reasonable physically since the energy that emerges should consist of those photons emitted over the mean free path for escape. The rate of emission is j, and mean free path is 1/k, so it is reasonable that the intensity saturates to S=j/k. For $T \ll 1$, $e^{-T} \approx 1-T$, so $I = ST$. Here again the answer is sensible physically because in the optically thin case we can see through the entire volume. Thus the energy emitted (per unit area) must be the emissivity j times the total path length z through the volume. So,

$$I = jz = (j/k)(kz) = ST$$

In this limit we have recovered the equation (2.6).

Suppose now we consider an arbitrary interior point in an atmosphere of finite thickness T and apply the usual boundary conditions. Thus considering first the case of $\mu \geq 0$ i.e. outgoing radiation towards the observer, we have from equation (2.13)

$$I^{+}(\tau,\mu) = \lim_{\tau 2 \to T} I(\tau 2,\mu)e^{-(\tau 2-\tau)\phi/\mu} + \int_{\tau}^{T} S(t)e^{-\{(t-\tau)\phi/\mu\}}\phi/\mu \, dt$$

for $0 \leq \mu \leq 1$ ---------- (2.16)

or from boundary condition $T \to \infty$

$$I^{+}(\tau,\mu) = \int_{\tau}^{T} S(t)\, e^{-\{(t-\tau)\phi/\mu\}}\phi/\mu \, dt$$

---------- (2.17)

Considering now $\mu \leq 0$ i.e.radiation away from observer, we take $\tau_2 = 0$, so that,

$$I^{-}(\tau,-\mu) = I(0,-\mu)\, e^{-\tau\phi/\mu} + \int_{0}^{\tau} e^{-\{(\tau-t)\phi/\mu\}}\, \phi/\mu \, dt$$

$(0 \leq \mu \leq 1)$

---------- (2.18)

or from boundary condition (2.2)

$$I^{-}(\tau,-\mu) = +\int_{0}^{\tau} S(t)\, e^{-\{(\tau-t)\phi/\mu\}}\phi/\mu \, dt$$

$(0 \leq \mu \leq 1)$

---------- (2.19)

Equation (2.17) and (2.19) constitute the complete solution of the transfer equation if the source function $S(\tau)$ is given. After having obtained a formal solution of the transfer equation, we may now perform integration over the

angles to derive the specific intensity and to write the solution in a concise and useful form for escape probability formalism.

Making use of solution in equation (2.18) and (2.16) for more general purpose, we have,

$$J(\tau) = 1/2 \int_{-1}^{+1} I(\tau,\mu)\, d\mu$$

$$= 1/2 \int_{0}^{1}[I^{+}(\tau,\mu)e^{-(T-\tau)\phi/\mu} + \int_{\tau}^{T} S(t)e^{-(T-\tau)\phi/\mu}\phi/\mu\, dt]d\mu$$

$$+1/2\int_{-1}^{0}[I^{-}(0,-\mu)e^{-(\tau)\phi/\mu} + \int_{0}^{\tau} S(t)e^{-\{(\tau-t)\phi/\mu\}}\phi/\mu\, dt]d\mu$$

---------- (2.20)

Since t and μ are independent variables we can change the order of integration in the second term of parentheses. putting $w = 1/\mu$, so that $-d\mu/\mu = dw/w$. We get,

$$J(\tau) = 1/2\, I^{+}(\tau,\mu)\int_{1}^{\infty} e^{-w(T-\tau)\phi}\, dw/w^{2}$$

$$+ 1/2\int_{\tau}^{T} S(t)\phi\, dt \int_{1}^{\infty} e^{-w(t-\tau)\phi} dw/w + 1/2\, I^{-}(o,-\mu)\int_{1}^{\infty} e^{-w\tau\phi}$$

$$dw/w^{2} + 1/2 \int_{0}^{\tau} S(t)\phi dt \int_{1}^{\infty} e^{-w(\tau-t)\phi}\, dw/w$$ ---------- (2.21)

The integrals against w are of a well known form and are called the exponential integrals. In general, for integer values of n, one defines the nth exponential integral by the expression,

$$E_{n}(x) = \int_{1}^{\infty} e^{-xt}/t^{n} = x^{n-1}\int_{x}^{\infty} e^{-t}/t^{n} dt$$

Thus in terms of $E_1(x)$ and $E_2(x)$ equation (2.21) may be written as,

$$J(\tau) = 1/2\, I^{+}(\tau,\mu)E_{2}[(T-\tau)\phi] + 1/2\phi \int_{\tau}^{T} S(t)E_{1}[(t-\tau)\phi]\, dt$$

$$+ 1/2\, I^{-}(0,-\mu)\, E_{2}(\tau\phi) + 1/2\, \phi \int_{0}^{\tau} S(t)\, E_{1}[(\tau-t)\phi]\, dt$$

---------- (2.22)

Now re-introducing the frequency subscript equation (2.22) may be written as, and replacing $I^{+}(\tau,\mu)$ and $I^{-}(o,-\mu)$ by $I_\nu(\tau_\nu)$ and $I_\nu(0)$ respectively, we have,

$$J_\nu(\tau_\nu) = 1/2\ I_\nu(\tau_\nu)\ E_2[(T_\nu-\tau_\nu)\phi_\nu(x)] + 1/2\ I_\nu(0)E_2[(\tau_\nu\phi_\nu(x)] + 1/2\ \phi_\nu(x)\int_0^{\tau_\nu} S_\nu(t)\ E_1[(\tau_\nu-t)\phi_\nu(x)]dt + 1/2\ \phi_\nu(x)\int_{\tau_\nu}^{T_\nu} S_\nu(t)\ E_1[(t-\tau_\nu)\phi_\nu(x)]\ dt \quad \text{---------- (2.23)}$$

Now the profile function can be normalised as follows,

$$\int_{-\infty}^{+\infty} \phi_\nu(x)\ dx = 1 \quad \text{---------- (2.24)}$$

Using equation (2.24) and (2.23) takes the form,

$$J_\nu(\tau_\nu) = 1/2\ I_\nu(\tau_\nu)\int_{+\infty}^{+\infty} \phi_\nu(x)\ E_2[(T_\nu-\tau_\nu)\ \phi_\nu(x)]\ dx + 1/2\ I_\nu(0)\ \int_{-\infty}^{\tau_\nu} \phi_\nu(x)\ E_2[(\tau_\nu-t)\ \phi_\nu(x)]\ dx + 1/2\ \int_0^{\tau_\nu} S_\nu(t)\ dt \int_{-\infty}^{+\infty} \phi_\nu^2(x)\ E_1[(\tau_\nu-t)\ \phi_\nu(x)]\ dx + 1/2\int_{\tau_\nu}^{T_\nu} S_\nu(t)\ dt \int_{+\infty}^{+\infty} \phi_\nu^2(x)\ E_1[(t_\nu-\tau_\nu)\ \phi_\nu(x)]\ dx \quad \text{---------- (2.25)}$$

Combining the two integrals over t and writing the equation (2.25) in terms of Kernel functions K_1 and K_2 defined by Averret and Hummer (1965) we have,

$$J_{,,}(\tau_\nu) = 1/2\ I_\nu(0)\ K_2(\tau_\nu) + 1/2\ I_\nu(\tau_\nu)\ K_2(\tau_\nu-\tau_\nu) + \int_0^{T_\nu} K_1[\text{abs}(\tau_\nu-t)]\ S_\nu(t)\ dt \quad \text{---------- (2.26)}$$

where $K_1[\text{abs}(\tau_\nu-t)] = 1/2 \int_{-\infty}^{+\infty} \phi_\nu^2(x)\ E_1[\phi_\nu(x)\text{abs}(\tau_\nu-t)]\ dx$ ---------- (2.27)

$$K_2(t_\nu) = \int_{-\infty}^{+\infty} \phi_\nu(x)\ E_2[\phi_\nu(x)\tau_\nu]\ dx \quad \text{---------- (2.28)}$$

Equation (2.26) is the general solution for the local radiation field which can be used in either condition. Using the properties of exponential integrals one can write,

$$\int_0^{\tau_\nu} K_1(\tau_\nu - t)\, dt = 1 - 1/2\, K_2(\tau_\nu) - 1/2\, K_2(T_\nu - \tau_\nu) \qquad \text{---------- (2.29)}$$

Although in reality the homogeneous and isothermal clouds do not exist but this assumption will simplify the equation (2.26) as,

$$J_\nu(\tau_\nu) = \beta(\tau_\nu)\, I_\nu(0) + \beta(t_\nu - \tau_\nu) I_\nu(\tau_\nu) + S_\nu(\tau_\nu)[1 - \beta(\tau_\nu) - \beta(T_\nu - \tau_\nu)] \qquad \text{---------- (2.30)}$$

where $\beta(\tau_\nu) = 1/2\, K_2(\tau_\nu)$

This is defined as the probability that a photon emitted at τ_ν will escape the boundary.

As observationally has been found that most of the lines are optically thin therefore the assumption in TH model that total optical depth T_ν being ∞ is contrary to the observations. If $T_\nu \to \infty$ the equation (2.30) reduces to,

$$J_\nu(\tau_\nu) = I_\nu(0)\, \beta(\tau_\nu) + S_\nu[1 - \beta(\tau_\nu)] \qquad \text{---------- (2.31)}$$

This is the expression used by de Jong et.al. (1980) and Tielens and Hollenbach (1985). Thus in reality the expression (2.31) should not be employed for the interpretation of the observed line intensities from the PDRs or diffuse clouds when the lines are optically thin.

2.2 Ultraviolet Penetration Through PDR:

In the present model, we use the radiative transfer formalism of Boisse (1990) to compute the mean UV intensity as a function of depth z, into a two phase clumpy region. Although the expressions are general in nature, we apply them to the case of UV radiative transfer through a region of high density, low filling factor material(the clumps) and lower density, high filling factor material (the interclump medium). The derived solution comes in pairs: one for the average intensity in the clumps and one for the average intensity in the interclump medium. In our model, the clumps have sufficiently large opacities(A_v ~ few hundred) as to transmit little UV radiation and thus the radiaton incident on the clump(i.e. the interclump radiation) is the relevant intensity. Hence in this scenario the PDRs are located on only half of the clump surface, the half which is directly illuminated by the UV and throughout the interclump material. Illumination of the clumps on the back side via scattering of the UV photons is very small as compared to the front side and hence not too important.

According to Boisse (1990) the equation of radiative transfer for the case of isotropic scattering may be written as if suffix ν for frequency dependence is dropped,

$$\partial I(M,\theta,\phi)/\partial s = - K(M)\, I(M,\theta,\phi) + \omega K(M)\, J(M) \qquad \text{---------- (2.32)}$$

Where $I(M,\theta,\phi)$ is the specific intensity at point M along a distance s defined by the angle θ and ϕ, J(M) the mean intensity (average of I over θ and ϕ), K(M) the extinction coefficient and ω the albedo of dust grains.

Assuming a plane parallel geometry with a uniform K(M) between the planes z = 0 and z = L [K(M) = 0 outside] and incident photons travelling to the OZ axis.fig (2.1). By integration of equation (2.32) over s and all directions (θ,ϕ) the classical integral equation for J can be written as,

$$J(z) = \phi_{in}/4\pi \exp(-Kz) + \omega K/2 \int_0^L E_1(K|z-z'|)\, J(z')\, dz' \qquad \text{---------- (2.33)}$$

in which ϕ_{in} is the incident flux and $E_1(x)$ the first order exponential integral function. The contribution to the J at any point in the medium comes from the incident photons and scattered photons from the clump and interclump medium. The contribution from the photons which have undergone no interaction is taken as $J^o(z)$, and $J^s(z)$ represents the sum over the whole layer of all scattered photons.

The fluxes on a plane normal to OZ in the direction of incident photons $\phi^+(z)$ or in the opposite direction $\phi^-(z)$ are given by the following expression, once J(z) has been obtained from equation (2.33) then flux at any point z inside the medium for the direction of incident photon and its opposite direction may be written as,

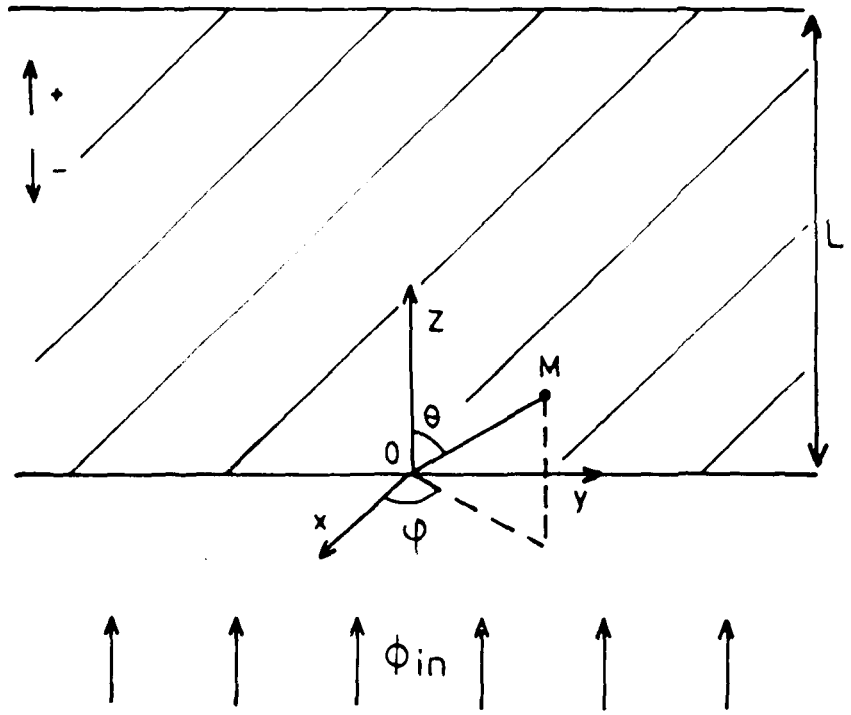

Fig. 2.1 : Geometrical representation of the plane parallel slab illuminated by the FUV radiation.

$$\phi^{+}(z) = \phi_{in}\exp(-Kz) + 2\pi\,\omega\,K\int_{0}^{z}E_2[K|z-z'|\,J(z')\,dz'$$

---------- (2.34)

and

$$\phi^{-}(z) = 2\pi\,\omega\,K\int_{z}^{L}E_2[K|z-z'|]\,J(z')\,dz'$$

---------- (2.35)

Here E_2 denoting the second order exponential integral function.

Boisse assume that extinction coefficient K(M) is a random function of position M which may take two values: K_0 inside clumps and K_1 outside (then unless stated, $K_1<K_0$) with respective probabilities P_0 and $P_1= 1-P_0$ (P_0 is then the volume filling factor of the clumps and P_1 for interclump)

In the frame of the Merkov model, the main overall characteristics of the medium can be computed. The average opacity over a distance L is,

$$\langle\tau\rangle = P_0K_0L + P_1K_1L = \langle K\rangle L$$

$$\langle K\rangle = P_0K_0 + P_1K_1$$

The contribution to the average phtotons at any point in the medium comes from the incident photons and scattered photons from the clump and interclump medium. Thus we have a couple of integro-differential equation which can be solved using Laplace transformation as has been done by Boisse (1990). The $\mathcal{L}(\langle J_0^{(0)}\rangle)$ and $\mathcal{L}(\langle J_1^{(0)}\rangle)$ are Laplace transform of $J_0^{(0)}$ and $J_1^{(0)}$ respectively which can be written,

$$\mathcal{L}(\langle J_0^{(0)}\rangle) = J_{in}\,(k+\nu+K_1)/[k^2+(\nu+K_0+K_1)k+\nu(P_0K_0+P_1K_1)+K_0K_1]$$

and a similar expression for $\mathcal{L}(\langle J_1^{(0)}\rangle)$ (k is the conjugate variable of z). Denoting the zeroes of the second order polynomial in the denominator by $-k'$ and $-k''$ (with $0<k'<k''$) we have

$$k'^{(")} = 1/2\ (\nu + K_0+K_1-(+)\ [(\nu+K_0+K_1)^2-4\ \nu<K>-4K_0K_1]^{1/2})$$

and finally obtain,

$$\langle J_0^{(0)}(z)\rangle = J_{in}[(\nu+K_1-k')\ \exp(-k'z) + (k''-\nu-K_1)\exp(-k''z)]/(K''-K') \quad \text{---------- (2.36)}$$

$$\langle J_1^{(0)}(z)\rangle = J_{in}[(\nu+k_0-k')\ \exp(-k'z) + (k''-\nu-K_0)\ \exp(-k''z)]/(K''-K') \quad \text{---------- (2.37)}$$

The average over both faces is simply given by,

$$\langle J^{(0)}(z)\rangle = P_0\langle J^{(0)}(z)\rangle + P_1\langle J^{(0)}(z)\rangle$$

Following Boisse (1990) the photon flux at any point z in the clump and interclump medium can be writen as,

$$\langle J_0(z)\rangle = \omega\ K_0/2(k''-k')\int_0^L F_{00}(z-z')\ \langle J_0(z')\rangle dz' + \omega\ K_1/2(k''-k')\int_0^L F_{01}(z-z')\ \langle J_1(z')\rangle dz' + \langle J_0^{(0)}(z)\rangle \quad \text{---------- (2.38)}$$

$$\langle J_1(z)\rangle = [\omega\ K_0/2(k''-k')]\ \int_0^L F_{10}(z-z')\ \langle J_0(z')\rangle\ dz' + [\omega\ K_1/2(k''-k')]\int_0^L F_{11}(z-z')\ \langle J_1(z')\rangle dz' + \langle J_1^{(0)}(z)\rangle \quad \text{---------- (2.39)}$$

where,

$$F_{00}(x) = (\nu p_0+K_1-k')\ E_1(k'|x|) + (k''-\nu p_0-K_1)\ E_1(k''|x|)$$

$$F_{01}(x) = \nu P_1[E_1(k'|x|) - E_1(k''|x|)]$$

$$F_{10}(x) = \nu P_0[E_1(k'|x|) - E_1(k''|x|)]$$

$$F_{11}(x) = (\nu p_1 + K_0 - k')\, E_1(k'|x|) + (k'' - \nu P_1 - K_0)\, E_1(k''|x|)$$

Once $\langle J_0 \rangle$ and $\langle J_1 \rangle$ have been computed, $\langle J \rangle$ is readily obtained ($\langle J \rangle = P_0\langle J_0 \rangle + P_1\langle J_1 \rangle$) as well as the angular dependence of the radiation.

The solutions for the equations (2.38) and (2.39) can be obtained through iterative procedure. The initial value for photons are calculated from equations (2.36) and (2.37). Then successive values of $J_0(z)$ and $J_1(z)$ are fed in till the solution is stabilized. These values of J_0 and J_1 are used for calculation of $\phi_i^+(z)$ and $\phi_i^-(z)$ (here i = 0 or 1 for clump and interclump), the flux in the direction of propagation and in opposite direction. The equation for ϕ^+ and ϕ^- are given as follows,

$$\langle \phi_i^+(z) \rangle = [2\pi\, \omega\, K_i/(k''-k')] \int_0^z G_{ii}(z-z')\, \langle J_i(z') \rangle\, dz' + [2\pi\, \omega\, K_j/(k''-k')] \int_0^z G_{ij}(z-z')\, \langle J_j(z')\, dz' + \langle \phi_i^{(0)}(z) \rangle \qquad \text{---------- (2.40)}$$

and

$$\langle \phi_i^-(z) \rangle = [2\pi\, \omega\, K_i/(k''-k')] \int_z^L G_{ii}(z'-z)\, \langle J_i(z') \rangle\, dz' + [2\pi\, \omega\, K_j/(k''-k')] \int_z^L G_{ij}(z'-z)\, \langle J_j(z') \rangle\, dz' \qquad \text{---------- (2.41)}$$

Where $\langle \phi_i^{(0)} \rangle$ is the flux of unscattered photons ($\langle \phi_i^{(0)} \rangle = 4\pi\, \langle J_i^{(0)} \rangle$; The functions G_{ii} and G_{ij} have similar expressions as the F_{ii} and F_{ij} previously introduced except for the fact that $E_2(x)$ (the second order exponential

integral function) now replaces $E_1(x)$. *Hence,*

$$G_{ii} = (\nu P_i + K_j - k') E_2[k'(x)] + (k'' - \nu P_i - K_j) E_2(k''x)$$

2.3 Reduction of Non Homogeneous Problem to Homogeneous One:

The situation can be obtained by imposing the condition that $K_o = K_1 = K$, and $P_i = 0$ (i.e. $P_j = 1$). It means there is no distinction between clump and interclump. Then $J_o(z)=J_1(z)$ and $k' = K$ and $K'' = \nu + K$.

These values when substituted into equations for G_{ii} and G_{ij} of equations (2.40) and (2.41) gives,

$$G_{oo} = \nu E_2 (K|x|)$$

$$G_{o1} = 0$$

$$G_{1o} = \nu [E_2(K|x|) - E_2(K''|x|)]$$

$$G_{11} = \nu E_2(K''|x|)$$

This reduces the equation (2.40) and (2.41) for forward and backward fluxes respectively, emitted over hemisphere as,

$$\langle \phi_i^+(z) \rangle = 2\pi\omega k \int_o^z E_2(K|z-z'|) \langle J(z') \rangle dz' + \phi_{in} \exp(-Kz)$$

---------- (2.42)

$$\langle \phi_i^-(z) \rangle = 2\pi\omega K \int_z^L E_2[K|z-z'|] \langle J(z') \rangle dz'$$

---------- (2.43)

which is same as equation (2.34) and (2.35).

2.4 Physical Parameters and Assumptions:

The PDRs/molecular clouds in the TH model are homogeneous, one dimensional semi infinite plane parallel slab illuminated on the finite side by FUV radiation in which inward directed photons can not escape. But it has been

observed that mostly FIR and sub millimeter radiation (line and continuum both) are optically thin hence radiation can escape at both the ends. To account these facts in one dimensional approach the PDRs are assumed to be finite plane parallel slab and accordingly the mathematical formulations are made and are discussd above. In order to study the effects of the present formalism clumpy structure of M17 region is considered. In the recent past a great deal of work have been done on M17 by Miexner et.al. (1992), Boreiko and Betz (1991), Stutzki et.al. (1988), Harris et.al. (1987), Rainey et.al. (1987), Schulz and Krugel et.al. (1987), Zmuidzinas et.al. (1986), Keene et.al. (1985), and Thronson et.al. (1983). In order to study M17 we are taking the flux G_o=5.6 x 10^4 times more intense the radiation field (1.2 x 10^{-4}ergs cm^{-2} $s^{-1}sr^{-1}$) of Habing (1968). Further density of clump and interclump in which clump is assumed to be embeded are taken as free parameters varied over a wide range ($100 \leq N \leq 10000000$). The turbulent velocities for interclump and clump are taken as 7.8 and 1.5 Kms^{-1} as found from observations.

The ultraviolet flux will be attenuated during the penetration deep into the cloud because of dust and also influenced by the absorption of neutral atoms and molecules. The attenuation of FUV radiation by the dust is proportional to exp ($-\tau_{uv}$) where τ_{uv} is the ultraviolet optical depth for

($912 \leq \lambda \leq 2100^{o}$A). The optical depth parameter depends upon the extinction coefficient K_{ν} and depth z in the cloud from the boundary i.e. interface of HII /HI and they are related as follows,

$$\tau_{uv} = K_{\nu} z$$

for the present study we use,

$$\tau_{uv} = 4.2 \times 10^{-9} N z(1000/\lambda)$$

given by Miexner and Tielens (1993). The depth z is in pc. wavelength in angstrom and N is the number density. Further the absorption of radiations by neutral carbon, CO and H_2 has important bearing in the CII, CI, CO, HI, and H_2 abundances inside the medium. The depth of penetration of UV radiation is dependent of the abundances too. For the present calculation the abundances of differnt species have been taken from Tielens and Hollenbach (1985). Further for abundance structure of neutral, ionic and molecular species a detailed chemical equilibrium is solved under steady state conditions.

CHAPTER - 3

ABUNDANCE CALCULATION

CHAPTER - 3

ABUNDANCE CALCULATION

The gas phase processes responsible for the formation of the simplest Carbon, Oxygen, and Nitrogen bearing molecules were identified about 15 years ago and have been discussed extensively e.g. by Dalgarno and Black (1976), Dalgarno (1976a) and Watson (1978). Recent reviews of cloud chemistry with a large number of refrences have been given by Crutcher and Watson (1985), Dalgarno (1988) and Vandishoeck and Black (1988a).

Although varieties of molecular reactions can take place in the interstellar clouds but only those reactions are considered here which have an important bearing on the molecular formation/destruction in the interstellar clouds. It has been observed that the amount of molecules in diffuse cloud is small because they are rapidly photodissociated by the interstellar radiation field. This process also severely limits the building up of more complex molecules. Mostly atomic content and the importance of photodissociation make diffuse cloud chemistry significantly different from the dark cloud chemistry. Thus it is quite clear that not only interstellar radiation field but atomic and dust content too play an important role in the chemistry of clouds. The distinction between diffuse and dark clouds is most

conveniently described in terms of the extinction coefficient A_v at visible wavelengths. Diffuse clouds have A_v less than about 2 magnitudes, where as dark clouds often have $A_v > 10$ mag. So that ultraviolet photons do not penetrate to the centers of dark clouds.

Further in order to solve for the abundances of diferent molecular, atomic and ionic species apart from the cloud chemistry some other atomic and molecular processes are also important. These are taken into account when we solve for the concentrations of species assuming chemical equilibrium to be established in the medium. For the chemical equilibrium we write as,

$$R\, n_i = D\, n_j$$

where R and D are formation and destruction mechanism for the species i & j respectively with number density n.

In the following the individual networks for species containing oxygenn, carbon and nitrogen are discussed.

3.1 Chemistry of Interstellar Gas:

To describe the chemistry of interstellar clouds detailed networks of reactions can be built based on the different types of processes of molecule formation. The most important reactions in the gas phase formation are of simple Carbon, Oxygen and Nitrogen containing molecules.

The schematic diagrams of the Carbon, Oxygen, Nitrogen and Sulphur chemistries are shown in the diagrams 3.1, 3.2,

3.3 and 3.4 respectively. It is evident from the networks shown in the diagrams that there are number of processes which lead to the formation of molecules in different conditions. But all pathways of molecule formation are not equally favourable. Only those processes which are most favourable for the formation of simple molecules in dense and diffuse clouds are discussed below.

The most important step for the initiation of Carbon chemistry is the formation of H_2 molecule by gas phase/gas-grain chemistry. Once H_2 is formed the formation of Carbon bearing molecules in diffuse as well as dense clouds is started by the radiative association of the abundant C^+ ion with H_2

$$C^+ + H_2 \longrightarrow CH_2^+ + h\nu \quad \text{---------- (3.1)}$$

chemical reactions leading to the formation of simple hydrocarbons, such as CH, CH^+, CH_2, CH_3, CH_4, C_2, C_2H_2 can be easily seen from the diagram (3.1). Cosmic ray ionization of both H and H_2 produces H^+ and H_2^+ ions. Endothermic charge transfer reaction between H^+ and O

$$H^+ + O \longrightarrow H + O^+ \quad \text{---------- (3.2)}$$

leads to the formation of the O^+ ions needed to start the Oxygen chemistry in diffuse clouds via the reaction chains,

$$OH_2^+ + e^- \longrightarrow OH + H \quad \text{---------- (3.3)}$$

$$OH_3^+ + e^- \longrightarrow H_2O + H \quad \text{---------- (3.4)}$$

$$\longrightarrow OH + H_2 \quad \text{---------- (3.5)}$$

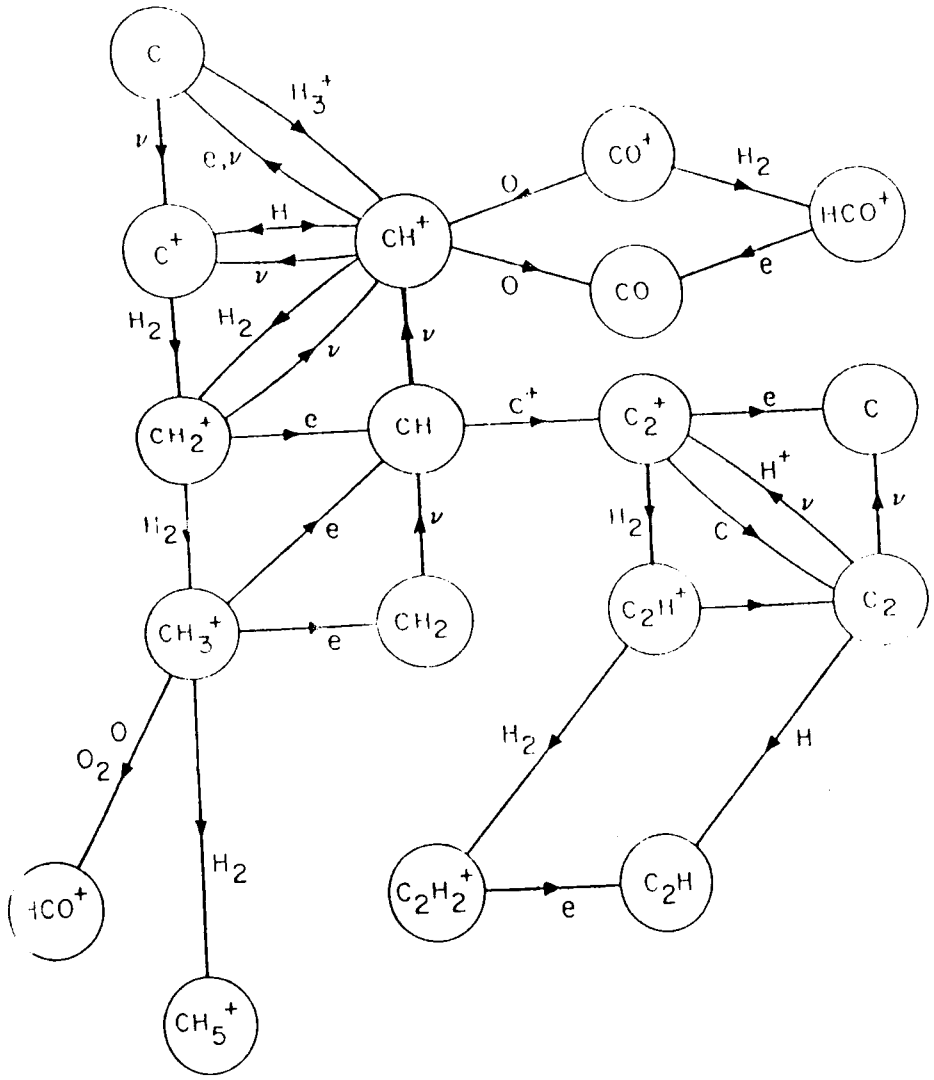

Diagram 3.1 : A simplified version of Carbon chemistry.

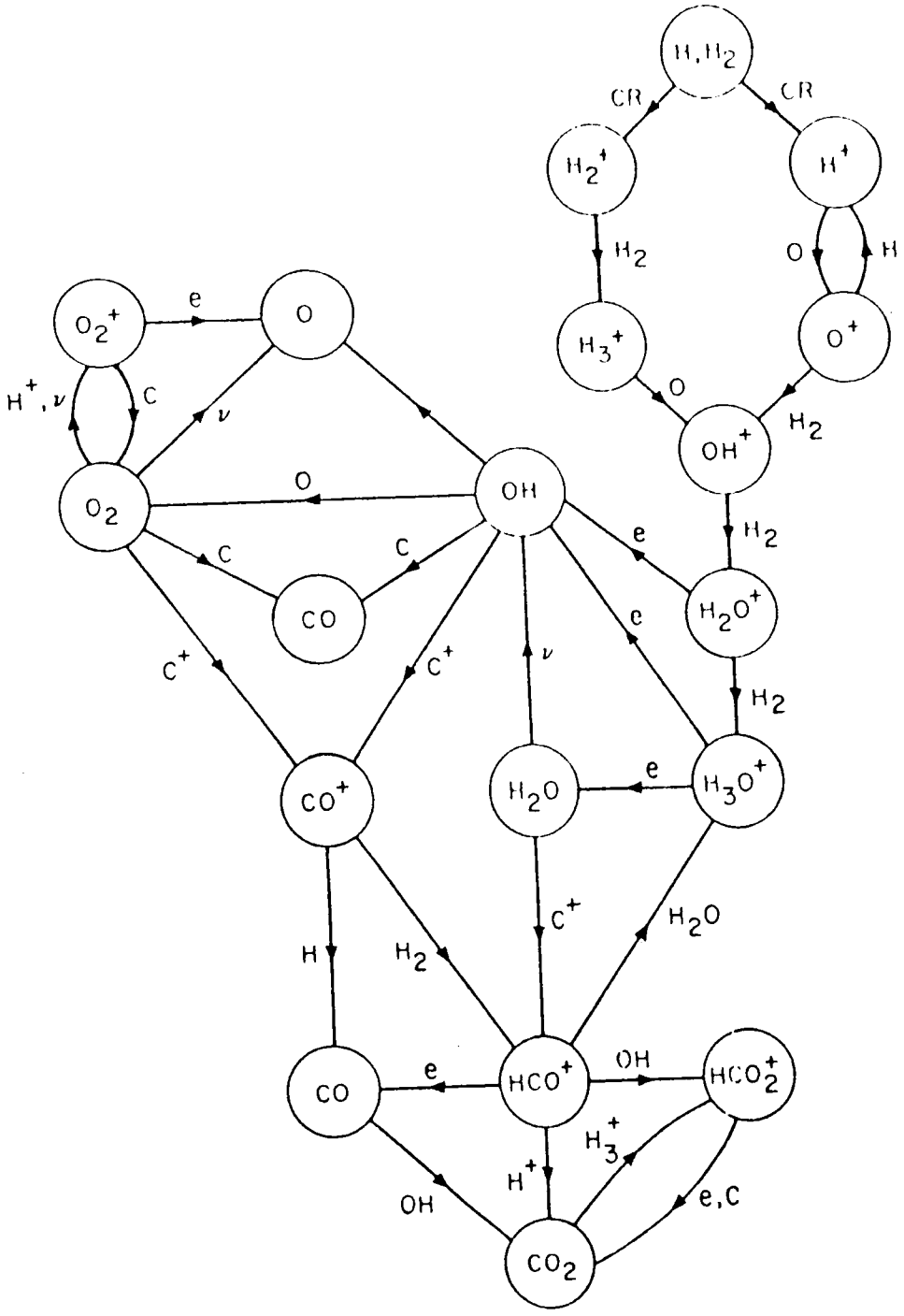

Diagram 3.2 : A simplified version of Oxygen chemistry.

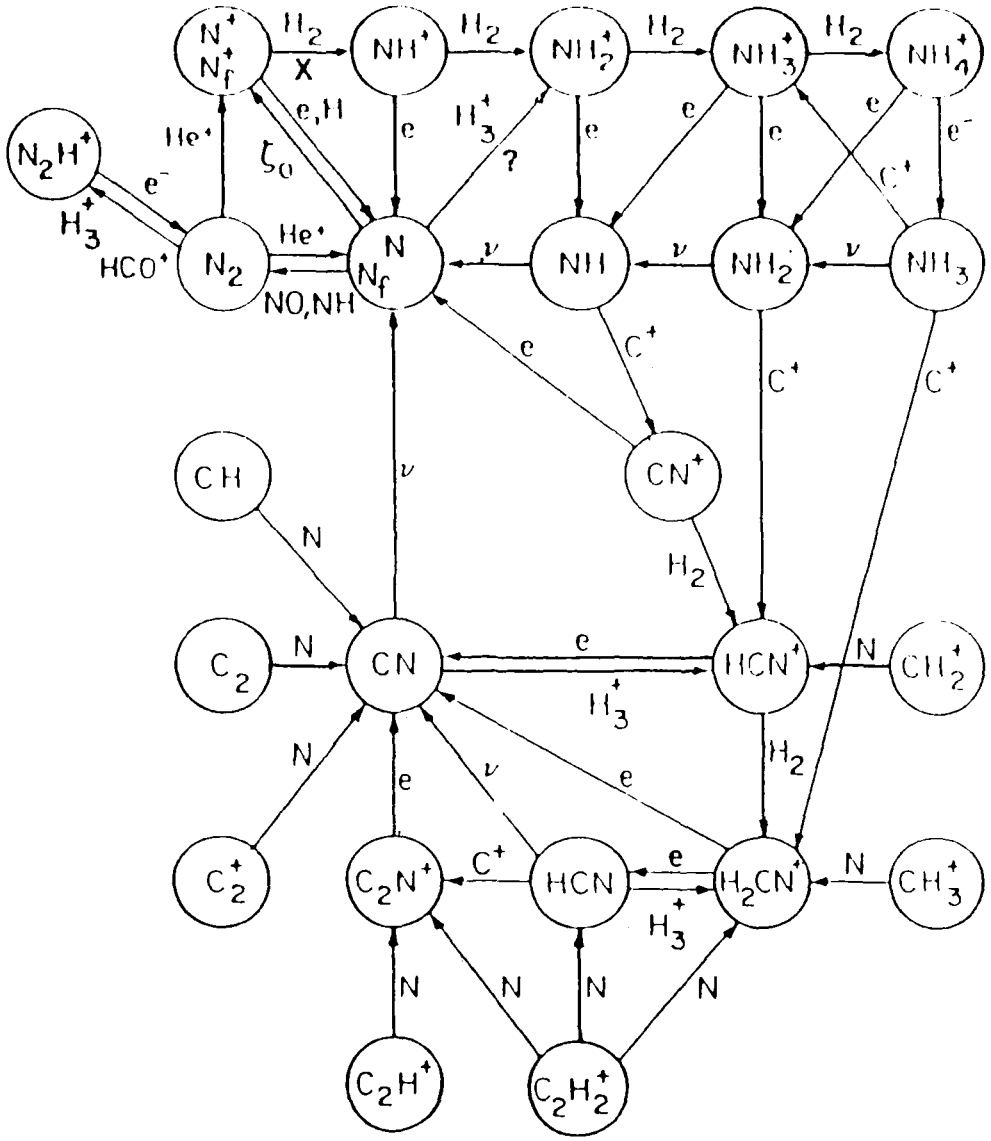

Diagram 3.3 : A simplified version of Nitrogen chemistry.

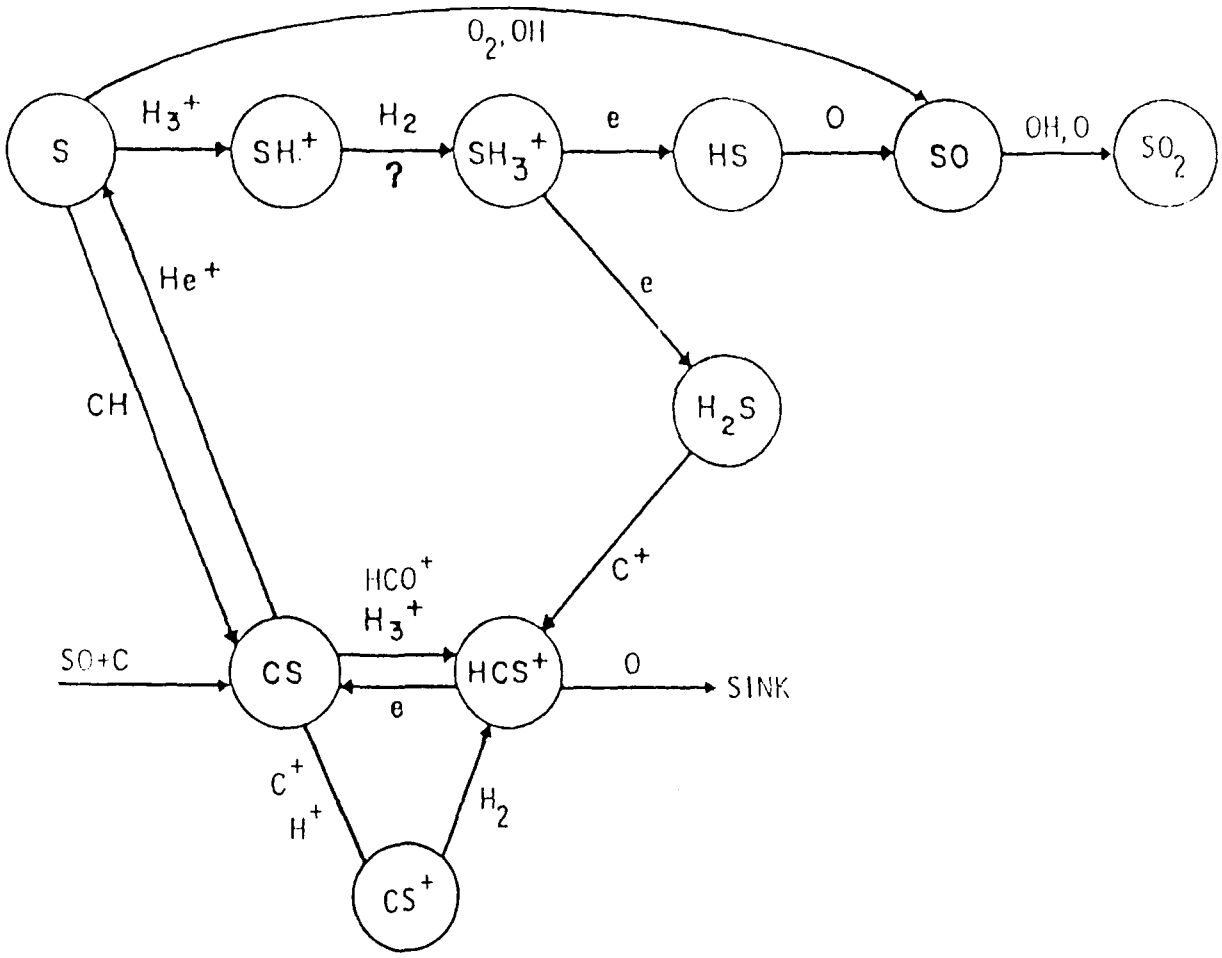

Diagram 3.4 : A simplified version of Sulphur chemistry.

$$H_2O + h\nu \longrightarrow OH + H \qquad \text{---------- (3.6)}$$

Since the energy of UV photons is not sufficient to ionize the Oxygen and O^+ ions can not be produced by the photoionization of O in interstellar clouds. The production of O^+ ions by the reaction (3.2) is quite sensitive to the cloud temperature due to endothermicity of the reaction. Consequently, the OH and H_2O concentrations in the clouds are also sensitive to the cloud temperature. From diagram (3.2) the important routes of the formation of OH and H_2O are,

$$O^+ + H_2 \longrightarrow OH^+ \xrightarrow{H2} H_2O^+ \xrightarrow{H2} H_3O^+ \xrightarrow{e^-} H_2O \qquad \text{---------- (3.7)}$$

and

$$H_2O^+ \xrightarrow{e^-} OH \qquad \text{---------- (3.8)}$$

$$H_3O^+ \xrightarrow{e^-} OH \qquad \text{---------- (3.9)}$$

In diffuse interstellar clouds with A_v less than 2 mag. the principal source of CO is the reaction

$$C^+ + OH \longrightarrow CO + H^+ \qquad \text{---------- (3.10)}$$

$$\longrightarrow CO^+ + H \qquad \text{---------- (3.11)}$$

where reaction (3.11) is followed by,

$$CO^+ + H_2 \longrightarrow HCO^+ + H \qquad \text{---------- (3.12)}$$

$$HCO^+ + e \longrightarrow CO + H \qquad \text{---------- (3.13)}$$

In dense clouds reactions such as,

$$C^+ + H_2O \longrightarrow HCO^+ + H \qquad \text{---------- (3.14)}$$

$$CH_3^+ + O \longrightarrow HCO^+ + H_2 \qquad \text{---------- (3.15)}$$

$$CH + O \longrightarrow CO + H \qquad \text{---------- (3.16)}$$

also contribute to the formation of CO.

Synthesis of the H_3^+ ions via the ion-molecule reaction (shown in diagram 3.2),

$$H_2^+ + H_2 \longrightarrow H_3^+ + H \qquad \text{---------- (3.17)}$$

is one of the most crucial steps in the interstellar chemistry, because H_3^+ ion plays innumerable pivotal roles in the molecular evolution. For example, in the dark clouds, where the endothermic reaction (3.2) can not occur and C^+ abundance is very small, the Oxygen and Carbon chemistries are initiated by the H_3^+ ions via the reaction;

$$O + H_3^+ \longrightarrow OH^+ + H_2 \qquad \text{---------- (3.18)}$$

$$C + H_3^+ \longrightarrow CH^+ + H_2 \qquad \text{---------- (3.19)}$$

The gas phase reactions through which Nitrogen containing molecules can be formed in diffuse as well as dense clouds are illustrated in diagram (3.3). They include neutral-neutral reaction of atomic nitrogen with small oxygen and carbon-containing molecules. Such as OH, CH, and C_2, CN and NO, and ion molecule reactions of atomic nitrogen with small hydrocarbon ions to foim e.g. H_2CN^+, which can then recombine to form CN and HCN. The important reactions in the formation of the above mentioned molecules are,

$$OH + N \longrightarrow NO + H \qquad \text{---------- (3.20)}$$

$$CH + N \longrightarrow CN + H \qquad \text{---------- (3.21)}$$

$$C_2 + N \longrightarrow CN + C \qquad \text{---------- (3.22)}$$

$$C_2^+ + N \longrightarrow CN + C^+ \qquad \text{---------- (3.23)}$$

$$C_2H^+ \xrightarrow{N} C_2N^+ \xrightarrow{e^-} CN \quad \text{---------- (3.24)}$$

and the routes of HCN formation are,

$$CH_2^+ \xrightarrow{N} HCN^+ \xrightarrow{H_2} H_2CN^+ \xrightarrow{e^-} HCN \quad \text{---------- (3.25)}$$

$$CH_3^+ \xrightarrow{N} H_2CN^+ \xrightarrow{e^-} HCN \quad \text{---------- (3.26)}$$

$$CH_3 + N \longrightarrow HCN + H_2 \quad \text{---------- (3.27)}$$

$$CH_2 + N \longrightarrow HCN + H \quad \text{---------- (3.28)}$$

$$C_2H_2^+ + N \longrightarrow HCN + CH^+ \quad \text{---------- (3.29)}$$

Ammonia (NH_3) and hydrogencynide (HCN), found mostly in the dense regions shielded from UV, are two important molecules. The formation of NH_3 is initiated by the following reactions.

$$N^+ + H_2 \longrightarrow NH^+ + H \quad \text{---------- (3.30)}$$

$$N + H_3^+ \longrightarrow NH_2^+ + H \quad \text{---------- (3.31)}$$

As with the nitrogen, significant processing of sulpher occurs only in the shielded regions where SO, SO_2, CS, HCS^+, OCS and H_2S have been observed in a number of clouds. Important reactions involved in their productions are shown in diagram (3.4)

3.2 Abundance Structure:

Following the Meixner and Tielens (1993) a test calculation has been performed to study the UV penetration into the clumpy cloud. The standard clump parameters are n_c(clump density) = 5 x 10^5 cm^{-3} and P_c= 0.2, while n_{ic}(inter clump density) is taken to be 300 cm^{-3} and 3000 cm^{-3}(Meixner

and Tielens 1993). For the standard clumpy case with n_{ic} = 300 cm^{-3}, the effective extinction coefficient (K_r) is 2 pc^{-1} and the effective albedo (ω_e) is 0.42, whereas, for n_{ic} = 3000 cm^{-3} they are 10 pc^{-1} and 0.70 respectively. The values of extinction coefficient and albedo for homogeneous ($n=10^5$ cm^{-3}) medium are 420 pc^{-1} and 0.76 respectively. The calculations reproduce the results of Miexner and Tielens (1993).

It is observed that UV radiation penetrates the clumpy region by an order of magnitude or more than in the homogeneous model ($n=10^5$ cm^{-3}). As evident from Boisse's work, the density of the clumps and thus the volume filling factor, has only a moderate effect on the penetration of the UV field (except in the limit P_c=1), while the interclump medium parameters have an enormous effect. Since an individual clump is highly optically thick in the UV (τ_{UV}=500), the UV penetration deep into the region is achieved by scattering through the interclump medium. In essence, the photons seep around the clumps through the interclump medium.

The net effect of the deep UV penetration into the region is that the column density of C and CO along a particular line of sight will be reduced, while the spatial extent of C^+ will be enhanced. As a result column density of C^+ will be increased. As the UV radiation penetrates farther

into the region it photoionizes more and more carbon and prevents the formation of CO, depleting the $C^+/C/CO$ transition zone.

Thus it is quite clear that clump structure of the cloud permits the penetration of UV radiation deep into the cloud, thus extending the CII region. But deep inside the cloud the abundances of almost all the molecules remain unaffected if compared with that of homogeneous cloud. The detailed abundance structure has not been discussed or shown here because sufficient efforts have already been made in this direction in the last decade.

Further the escape probability formalism has a little effect on the abundance structure that enter through the temperatutre dependent chemical reactions. Deep into the cloud where optical depth is large enough this dependence too vanishes.

Presently a model intensity calculation for the cloud M17 has been carried out and is reported in the fifth chapter The calclations are carried out assuming clump density = 6 x 10^5 cm^{-3} and interclump density = 4 x 10^3 cm^{-3} which are found to be the best fit densities of clump and interclump medium. The clump structure of M17 explains the extended CII emission and also enhanced line intensities of OI (63μm), SiII (35μm) and some rotational transitions of CO molecules as well. The turbulent velocities associated with clump and

interclump medium are 1.5 Km/s and 7.8 Km/s respectively which are representative observed values for the region.

CHAPTER - 4

THERMAL STRUCTURE

CHAPTER - 4

THERMAL STRUCTURE

4.1 Heating Mechanisms

4.1.1 Photoelectric Emission from Dust Grains:

Absorption of a FUV photon by a dust grain can give rise to the emission of an electron. The energy difference between the photon energy and the work function of the grain will be carried away in the form of kinetic energy by the electron. The energy carried by the electron is deposited in the medium through the interaction with the gas and as a result the medium gets heated.

Because the work function of the grain depends on its charge, the calculation of the net photoelectric heating rate is involved. Following de Jong (1977,1980), one can write for the net photoelectric heating rate,

$$\Gamma_1 = 2.7\times10^{-5}\delta_{uv}\delta_d n_o y G_o e^{-k_{uv}A_v}\,[(1-x^2)/x+x_k(x^2-1)/x^2] \quad \text{ergs cm}^{-3}\ \text{s}^{-1} \qquad \text{---------- (4.1)}$$

Where δ_{uv} is the ratio of the geometrical cross section of the grains that absorb in the FUV to that of the grains that absorbs in the visual, δ_d is the ratio of the dust abundance in these regions to that in the diffuse interstellar medium, n_o is the hydrogen nucleus density, y is the photoelectric yield of the dust grains, G_o is the mean

FUV flux incident on the slab in terms of that in the diffuse interstellar medium, and k_{uv} is the effective ratio of FUV optical depth to A_v, while x is grain charge parameter. By equating the photoelectric emission rate with the electron recombination rate of the grain yields an equation for the grain charge parameter x.

$$x^3 + (x_k - x_d + \gamma)x^2 - \gamma = 0 \qquad \text{---------- (4.2)}$$

where $x = \nu_o/\nu_h$, $x_k = KT/h\nu_H$, and $x_d = \nu_d/\nu_H$. Here T is the gas temperature, $h\nu_d$ is the photoelectric threshold energy for the neutral grain material, and $h\nu_o$ is the energy barrier which an elctron has to overcome, including the grain charge effect. The grain charge Z_d is then given by,

$$Z_d = (x-x_d)h\nu_H a/e^2 \qquad \text{---------- (4.3)}$$

where a is the grain radius.

The unitless parameter γ is given by,

$$\gamma = 2.9 \times 10^{-4} y T_o^{0.5} G_o e^{-k_{uv}A_v} n_e^{-1} \qquad \text{---------- (4.4)}$$

where n_e is the electron density in cm^{-3} and T is in K.

The photoelectric yield y and threshold $h\nu_d$ depend upon the grain material and the size of the grain particle (Watson 1972).

In the photodissociation region where carbon is predominantly in ionized form the cooling is mainly due to

CII. The comparable heating mainly comes through the photoemission from dust grains provided there are associated O/B stars providing high flux of UV i.e. G_o. It has been found that y= 0.1 and $h\nu_d$= 6eV are good approximations for the photoelectric yield and work function of the neutral grains inside the medium.

4.1.2 Heavy Element Ionization:

The absorption of UV photon by heavy elements gives photo electrons due to ionization which carries energy almost equal to the difference of photon energy and ionization limit of the element. Thus the net energy carried can be written as

$$\Gamma_2 = \int_{\nu_o}^{\nu} \sigma(\nu) F\ h(\nu-\nu_o)\ d\nu$$

---------- (4.5)

It is observed that in the medium of interest carbon is most abundant element. Therefore, heating here is considered only due to photoionization of carbon which after simplification can be written as follows (de Jong et.al.1980)

$$\Gamma_2 = 2.2 \times 10^{-22} n(c) G_o \exp(-2.4A_v - \tau_c - \tau b/\pi v_1^2) (1+\tau b/\pi v_1^2)^{-1} \text{ ergs cm}^{-3}\ s^{-1}$$

---------- (4.6)

where n(c) is the neutral carbon density. The first exponential factor in this equation describes the attenuation by dust absorption (Black and Dalgarno 1977), the second describes the attenuation by self absorption of C (Werner

1970), and the last describes attenuation by H_2 (de Jong, Dalgarno, and Boland 1980). The unitless parameters in this expression are given by,

$\tau_c = 10^{-17} N(c)$, $\tau = 1.2 \times 10^{-14} N(H_2) \delta v_d^{-1}$, $b = 9.2 \times 10^{-3} \delta v_d^{-1}$

and $v_1 = 5 \times 10^{2} \delta v_d^{-1}$ ---------- (4.7)

where N(c) and $N(H_2)$ are the column densities of neutral carbon and H_2, and δv_d is the turbulent Doppler line width in Km/s.

4.1.3 H_2 Photodissociation:

The pumping of H_2 molecules by photons in the Lyman and Werner bands can heat the gas through photodissociation. This occurs for about 10% of the pumps, when the radiative decay from the excited electronic state leads to the vibrational continuum of the ground electronic state. The total FUV pumping rate R_{pump} and the heating rate associated with photodissociation are given by,

$$R_{pump} = 3.4 \times 10^{-10} \beta(\tau)\, G_o\, e^{-2.5 A_v} \quad S^{-1} \qquad \text{---------- (4.8)}$$

$$\Gamma_3 = 1.36 \times 10^{-23} n(H_2) \beta(\tau) G_o e^{-2.5 A_v} \quad \text{ergs cm}^{-3}\ \text{s}^{-1} \qquad \text{---------- (4.9)}$$

where $n(H_2)$ is the number density of H_2 molecules in the ground state, and the exponential factors take dust absorption of FUV photons into account.

When photon absorption is dominated by the Doppler cores or Lorentz wings ($\tau > 10$), then the self shielding factor is

given by,

$$\beta(\tau) = \{\tau^{-1}[\ln(\tau/\pi)]^{1/2}+(b/\tau)^{1/2}\}\ \mathrm{erfc}(\tau b\pi^{-1}v_1^{-2})^{1/2} \quad \text{---------- (4.10)}$$

where τ, b, and v_1 are given by equation (4.7). In this expression line overlap has been taken into account. On the linear part of curve of growth, the self shielding factor is given by,

$$\beta(\tau) = \sum_{n=0}^{\infty} (-1)^n\tau^n/n!(n+1)^{1/2}\pi^{n/2} \quad \text{---------- (4.11)}$$

The latter equation for $\beta(\tau)$ is used for $\tau \leq 10$

4.1.4 Heating Due to H_2 Formation:

The formation of H_2 molecules on grain surfaces will lead to the heating of the medium. After their formation on grain surfaces the molecules enter the gas phase with an energy equal to their binding energy of 4.4 eV. A part of this energy raises the internal energy of H_2 as well as of grain, while the rest of the energy goes into as heat. The heating due to this process is

$$\Gamma_4 = R\, n_H\, n(H)\, Q_{H2}$$
$$= R(1-f)\, n_H^2\, Q_{H2} \quad \text{ergs cm}^{-3}\ \text{s}^{-1}$$

---------- (4.12)

where R is the molecular formation rate of H_2 and Q_{H2} is the fraction of energy converted to heat and f is the fraction of hydrogen molecules defined as $f = 2n(H)_2/n_H$. The total heating due to this process is uncertain because of uncertainty involved in the vlues of Q_{H2} and (1-f).

4.1.5 Gravitational Collapse:

A collapsing cloud can be heated by compression. Considering gravitational collapse at the free-fall rate of a molecular cloud of density n_H, temperature T, and pressure P, it is suggested that the compressional work per particle against the internal pressure P will be converted to heat and gives a heating rate,

$$\Gamma_5 = \rho P \, d/dt(1/\rho)$$
$$\approx 2.6 \times 10^{-31} T n_H^{1.5} \quad \text{ergs cm}^{-3} \text{ s}^{-1}$$

---------- (4.13)

For the present study of PDRs this process is not supposed to be significant in the heating of the cloud. As the mass associated with the PDRs are not so huge and free fall of these clouds is a distinct probability. So the heat generated by very slow compression can be neglected.

4.1.6 Heating Due to Gas Grain Collision:

An important heating source in some neutral regions of high density arises from collisions between gas molecules and dust grains that have been heated by the near infrared radiation field. An atom or molecule that strikes the surface of a grain at temperature T_d, comes into thermal equilibrium with that surface, and then re-enters the gas phase, may gain kinetic energy from the grain if $T_d > T$ or lose kinetic energy to it if $T > T_d$. The rate of heating and cooling depends upon the temperature difference, the frequency of

collision, the composition of the gas, the properties of the particular kind of solid, and the propensity of the atoms to stick to the surface. For the heating rate is given by,

$$\Gamma_{da} = [n(H)+n(H_2)]\, n_d \delta_d \bar{v}_H \bar{\alpha}_t\, (2KT_d - 2kT) \qquad \text{---------- (4.14)}$$

where $\bar{v}_H$ is the thermal speed of H atoms and $\bar{\alpha}_t$ measures the accomodation effect, where the average thermal accomodation coefficient $\bar{\alpha}_t$=0.3, appropriate for molecular gas at T ~ 100K colliding with grains at T_d ~ 100K. Inserting numerical values, we get

$$\Gamma_{da} = 3.5 \times 10^{-34}\, n^2\, \delta_d\, T^{1/2}\, (T_d - T) \text{ ergs cm}^{-3}\, s^{-1} \qquad \text{---------- (4.15)}$$

Similarly the gas is cooled by this process if $T > T_d$.

The dust temperature follows from the balance between photon absorption and emission,

$$4\pi a^2 \int_0^\infty Q_a(\nu)\pi B(\nu,T_d)\, d\nu = \pi a^2 \int_0^\infty Q_a(\nu) F(\nu) e^{-\tau(\nu)}\, d\nu + 4\pi a^2 \int_0^\infty Q_a(\nu)\, \pi\, J_d(\nu)\, d\nu \qquad \text{---------- (4.16)}$$

The last term describes absorption from the infrared emission of the dust. In this equation $Q_a(\nu)$ is the absorption efficiency of the dust and $J_d(\nu)$ is the mean radiation field due to dust. Assuming that,

$$Q_a(\nu) = \nu/10^{15}\ s^{-1}, \qquad \nu < 10^{15}\ s^{-1}$$
$$= 1 \qquad \nu > 10^{15}\ s^{-1},$$

and that the dust emission is characterized by a constant temperature T_o and total emission optical depth

$$\tau_d = \tau_{100\mu m} \quad (100\mu m/\lambda)$$

where $\tau_{100\mu m}$ is the 100μm emission optical depth. This yields the following equation for the dust temperature

$$T_d = \{8.8 \times 10^{-11} \nu_o G_o e^{-1.8A_v} + 2.7^5 + 3.4 \times 10^{-2}[0.42 - \ln(3.5 \times 10^{-2} \tau_{100} T_o)] \times \tau_{100} T_o^6 \}^{0.2}$$

Another way of heating the gas through the grains is radiation pressure which accelerates the grains relative to the gas and produces a viscous heating term due to gas drag. It is found that the grain acceleration time scale is short compared with other time scales, and the grains are moving at their local drift velocity v_d. Basically all the momentum gained by the grains through radiation pressure is transferred to the gas by, mainly coulomb drag. Typically the steady state drift velocity v_d is small ($<10^3$cm s^{-1}) in the calculation of heating rate, and no significant gas grain separation occures. The heating rate due to the grain drift is,

$$\Gamma_{gb} = 8\pi e^4 n_d Z_d (KT)^{-1} (\ln\Lambda) v_d [n(c^+)G(y_{CII}) + n_e G(y_e)] \qquad \text{---------- (4.17)}$$

where n_d is the grain number density, Z_d is the grain charge, $n(c^+)$ and n_e are the C^+ and electron number densities, and the functions Λ and G are given by,

$$\Lambda = 1.5\, Z_d^{-1} e^{-9} (KT)^{3/2} (\pi n_e)^{-0.5}$$

$$G = [erf(y) - 2ye^{-y^2}/\pi^{0.5}]/2y^2$$

where $y = v_d/v_{th}$, and v_{th} is the thermal velocity of the ion or electron.

4.1.7 Cosmic Ray Heating:

The determination of the heating rate due to cosmic rays is very complicated owing to the myriad processes by which the cosmic rays and their secondary ionization products lose energy. The heating efficiency is sensitive to the composition and density of the gas and to its degree of ionization. In a neutral molecular gas, the mean heating input per primary ionization (including the secondary processes) probably is about 8eV. The higher values apply at densities $n_H > 10^4$ cm^{-3}. Thus the cosmic ray heating rate in a molecular cloud is,

$$\Gamma_7 = 4 \times 10^{-28} (\zeta_p/4 \times 10^{-17})(\varepsilon_h/6ev) n(h_2) \text{ ergs cm}^{-3} \text{ s}^{-1}$$

---------- (4.18)

putting the numerical values it is given by,

$$\Gamma_7 = 1.5 \times 10^{-11}\, \zeta_p\, n(H_2) \quad \text{ergs cm}^{-3} \text{ s}^{-1}$$

---------- (4.19)

where ζ is the cosmic ray ionization rate per H_2 molecule.

4.2 Cooling Mechanisms:

The gas is generally cooled by the hyperfine transitions of atoms and ions especially CII(158μm), CI(370 and 609μm), OI(63 and 145μm), SiII(35μm), and rotational transitions of

CO(ΔJ = 1 to 20), its isotopes and some other molecules. The symbol for cooling is used as Λ(ergs $cm^{-3}s^{-1}$). The cooling is the function of population of different levels which enters also through the escape probability. To solve for level population statistical equilibrium equations are established (bound-bound) for m and n level species,

$$N_m \left(\sum_{l=1}^{n} P_{lm}\right) = \sum_{l=1}^{n} N_l P_{lm} \quad \text{---------- (4.20)}$$

for $l \neq m$

where N_m is the number density of the species in a level m and P_{lm} is the number density of transitions per atom between levels l and m per unit volume. The bound-bound rate coefficients are,

$$\left.\begin{aligned} P_{ml} &= A_{ml} + B_{ml}J_\nu + C_{ml} \\ P_{lm} &= B_{lm}J_\nu + C_{lm} \end{aligned}\right\} \text{for } m > l \quad \text{---------- (4.21)}$$

where ν corresponds to the frequency of m-l transitions. Here A and B are the Einstein's coefficients and C_{lm} and C_{ml} are the collisional excitation and de-excitation rates.

$$J_\nu = S_{ml}(\tau_\nu)[1-\beta(\tau_\nu)-\beta(T_\nu-\tau_\nu)] + \beta(\tau_\nu)I_\nu(0) + \beta(T_\nu-\tau_\nu)I_\nu(T_\nu) + \beta(\tau_\nu)\tau_d^\nu B(\nu,T_o) + \beta(T_\nu-\tau_\nu)\tau_d^\nu B(\nu,T_o)$$

---------- (4.22)

The source function S_{ml} is given by,

$$S_{ml} = 2h\,\nu_{ml}^3/C^2\,(g_m N_l/g_l N_m - 1)^{-1}$$

where g_m and g_l are the statistical weights of levels m and l, τ_d^ν is the dust optical depth at frequency ν. $B(\nu,T_o)$ is the infrared radiation at the temperature T_o.

Although equation (4.22) differs from that of THa but it can be recasted into the same form by defining total escape probability β_{esc} as follows

$$\beta_{esc} = \beta(\tau_\nu) + \beta(T_\nu - \tau_\nu)$$

Thus cooling efficiency will become as,

$$\Lambda_x(\nu_{ml}) = N_m A_{ml} h\nu_{ml} \beta_{esc}(\nu_{ml})[1-\beta(\tau_\nu)B/\beta_{esc}S_x(\nu_{ml})] \quad \text{---------- (4.23)}$$

The equations (4.22) and (4.23) differ from that of THa model because of different escape probability β_{esc} used here. This factor is very important here because it governs the cooling and also play an important role in level population for densities less than the critical density of the line.

Table 4.1 lists the atomic and ionic transitions included in the model. The collisional de-excitation rate coefficients γ_H for collisions with atomic hydrogen are given by the relation

$$\gamma_H = a\ T^b\ cm^{-3}\ s^{-1}$$

It is assumed that $\gamma_H = \gamma_{H2}$, except for C^+, where it is taken to be $\gamma_{H2} = 3.1 \times 10^{-10} T^{0.1}\ cm^{-3}\ s^{-1}$. The critical density n_{cr} is also given above which collisional de-excitation becomes important. Calculated with the assumption that the upper and lower levels forms a two level system. So that,

$$n_{cr} = A_{21}/\gamma_H \quad \text{---------- (4.24)}$$

4.2.1 Cooling Due to Atoms and Ions:

The contribution to the cooling from different species depends upon the conditions of the medium. If the temperature is high enough and the heavy elements are not depleted heavily then their contribution to the cooling may be significant, but it is found that in most of PDRs *temperature < 1000K. Therefore the cooling from the heavy* elements is not significant except that for SiII. The contribution of SiII cooling also becomes negligibily small when we proceed deep into the PDR because temperature falls rapidly.

Furthur in low temperature region cooling from carbon atom may be significant. But abundance structure shows that in the outer region carbon is mostly in the ionized form while deep into the cloud it is converted into CO molecules. Thus contribution to the cooling from neutral carbon is expected at CII/CI/CO interface in a very thin region.

The radiative cooling rate in a two level system like CII, which is most important coolant, due to transitions from level 2 to level 1 can be written as follows if we neglect the background radiation field,

$$\Lambda_{CII} = n_2 A_{21} \Delta E \beta \qquad \text{---------- (4.25)}$$

where n_2 is the population density of the upper state $^3P_{3/2}$, $A_{21} = 2.4 \times 10^{-6}$ is the Einstein's A coefficient, $\Delta E = 1.27 \times 10^{-14}$ ergs = 92K is the energy difference between the upper and lower states, and β is the escape probability of the

resulting 158μm photon. It is assumed that all carbon is ionized near the surface, thus $n_1+n_2 = n_{CII} = 3 \times 10^{-4} n_o$. To obtain n_2, the solution of a two level atom (Hollenbach and Mc Kee 1979) is used.

$$n_2/n_1 = g_2/g_1 \, e^{-\Delta E/KT} (1+\beta \, n_{cr}/n_o) \quad \text{---------- (4.26)}$$

where $g_1 = 2$ and $g_2 = 4$ are the statistical weights of the two energy levels. The critical density is given by equation (4.24) and γ_{21} is the collisional de-excitation rate coefficient for collisions with atomic/molecular hydrogen. Substituting the appropriate values one obtains,

$$\Lambda_{CII} = 9.14 \times 10^{-24} \, n_o \, \beta/[1+1/2 \, e^{92/T}(1+\beta \, n_{cr}/n_o)] \quad \text{---------- (4.27)}$$

If background field is present then the exact equation (4.23) is employed for calculation of cooling.

Using the data of table 4.1 the cooling rates of other atomic and ionic species can also be calculated.

4.2.2 Cooling By Molecular Lines:

The equation of statistical equilibrium equation (4.21) has already been discussed in detail. These equation are solved for population of different levels in multilevel system like molecules. In order to solve the statistical equilibrium one needs accurate collisional rates. The most important molecular coolant is CO molecule and its isotopes which are discussed here in little detail.

TABLE - 4.1
Atomic Fine Structure Data

species	Level g	Level u	E (K)	λ (μm)	A_{ul} (s^{-1})	a	b	n_{cr} (cm^{-3})	n_{τ} (cm^{-3})
Two Level Species									
C^+	$^2P_{1/2}$	$^2P_{3/2}$	92	157.7	2.4(-6)	5.8(-10)	0.02	2.8(3)	1.2(21)
Si^+	$^2P_{1/2}$	$^2P_{3/2}$	414	34.8	2.2(-4)	6.5(-10)		3.4(5)	4.6(23)
Three Level Species									
C	$^3P_0$	$^3P_1$	23.6	610	7.93(-8)	1.3(-10)	0.045	4.7(2)	4.2(20)
	$^3P_1$	$^3P_2$	38.8	370	2.68(-7)	7.8(-11)	0.035	2.8(3)	1.0(21)
	$^3P_0$	$^3P_2$	62.5	230	2.0(-14)	2.0(-10)	0.084	6.3(-5)	1.9(28)
O	$^3P_2$	$^3P_1$	228	63.2	8.95(-5)	4.2(-12)	0.67	4.7(5)	1.0(21)
	$^3P_1$	$^3P_0$	98	145.6	1.70(-5)	1.5(-10)	0.44	8.5(4)	7.8(20)
	$^3P_2$	$^3P_0$	326	44.0	1.0(-10)	1.1(-12)	0.8	9.7(-1)	8.0(27)
Si	$^3P_0$	$^3P_1$	111	129.6	8.25(-6)	3.5(-10)		2.4(4)	1.6(23)
	$^3P_1$	$^3P_2$	210	68.5	4.21(-5)	5.0(-10)		8.4(4)	3.8(23)
	$^3P_0$	$^3P_2$	321	44.8	3.56(-10)	1.7(-10)		2.1(0)	4.5(29)
S	$^3P_2$	$^3P_1$	571	25.2	1.39(-3)	7.5(-10)		1.9(6)	6.4(22)
	$^3P_1$	$^3P_0$	255	56.6	3.02(-4)	4.2(-10)		7.2(5)	4.7(22)
	$^3P_2$	$^3P_0$	826	17.4	6.71(-8)	7.1(-10)		9.5(1)	1.2(28)
Fe	$^5D_4$	$^5D_3$	595	24.2	2.5(-3)	8.0(-10)		3.1(6)	9.9(23)
	$^5D_3$	$^5D_2$	415	34.7	1.6(-3)	5.3(-10)		3.0(6)	5.7(23)
	$^5D_4$	$^5D_2$	1010	14.3	1.0(-10)	6.9(-10)		1.4(-1)	1.7(32)
Fe^+	$^6D_{9/2}$	$^6D_{7/2}$	554	26.0	2.13(-3)	9.5(-10)		2.2(6)	9.1(23)
	$^6D_{7/2}$	$^6D_{5/2}$	407	35.4	1.57(-3)	4.7(-10)		3.3(6)	5.2(23)
	$^6D_{9/2}$	$^6D_{5/2}$	961	15.0	1.5(-9)	5.7(-10)		2.6(0)	9.0(30)

The digits in parentheses should be read as powers of 10

Various assumptions have been made about the collision cross sectios that determine the coefficients $C_{jj'}$ in equation (4.20)[here the coefficients $_{lm}$ have been replaced by jj' following a general convention for molecular levels]. In the calculation of the populations of the rotational levels j of carbon mono-oxide, the required cross sections $\sigma(j-j')$ are those for the collisions,

$$H_2 + CO \longrightarrow H_2 + CO(j') \text{ ---------- } (4.28)$$

Goldsmith (1972) considered a variety of cross section estimates which varied slowly with j or j', were independent of energy, and were of the order of 10^{-15} cm^{-2}. Similar assumptions but with a cross section of 5×10^{-17} cm^{-2} were made by Glassgold and Langer (1973). Scoville and Solomon (1974) adopted the cross section derived by Compaan et.al. (1973) from measured widths of rotational Raman lines, which vary from 2.7×10^{-16} cm^{-2} for the 0-1 transitions to 6.6×10^{-17} cm^{-2} for the 0-5 transitions and are nearly independent of the initial rotational quantum number. Whereas Goldreich and Kwan (1974) assumed that for collisions in which

$$j' < j, \quad \sigma(j-j') = 2.5 \times 10^{-15} (hB/KT) cm^2 \text{ ---------- } (4.29)$$

where B is the rotational constant of CO. Garola and Sofia (1975) used cross section $\sigma(j-j') = 10^{-15}$ cm^2 and $\sigma(j-j') = 0$ depending upon the values of $(j-j')$.

de Jong et.al.(1975) based their selection of cross

sections on the close -coupling calculations of Green and Thaddeus (1975) who presents results $j \leq 5$ and $j' \leq 5$. They found that at the densities and temperatures of interest significant populations occured of the levels upto $j = 20$, therefore an extrapolation of the cross section data was required.

For the rate coefficients $K_{jj'}$ at temperatures T they adopted the empirical representation of the form,

$$K_{jj'} = a(\Delta J) g_{j'}/g_j (1+\Delta E_{jj'}/KT) \exp[-b(\Delta_j)(\Delta E_{jj'}/KT)^{1/2}] \quad \text{---------- (4.30)}$$

where $\Delta J = J-J'$, $E_{jj'} = hB[J(J+1)-J'(J'+1)]$ is the energy difference brtween levels j and j' and a and b are functions of Δj. Again for $\Delta j = \pm 1$, $\Delta E_{jj'} = 2hBJ$. the values of a and b for Δj upto 5 are represented in table 4.2. For further hyperfine transitions it is taken to be zero. In the present calculation level populations are solved for J = 20. Cooling rates are calculated using the general expression for cooling.

4.3 Temperature Structure

Mainly the cooling of PDR's, warm gas components and molecular clouds in the galactic and extra-galactic medium are due to the FIR and sub-millimeter line emission of CI(370 and 609 μm), OI(63 and 145μm), CII(158μm), SiII(35μm), FeII (26μm), and rotational lines of CO(ΔJ = 1 to 20) and its isotopes as well as luminous infra-red continuum from dust.

TABLE - 4.2

Constants "a" and "b" used in eqn.(4.30) of Collision Rate Coefficients K(j - j')

j-j'	$a(cm^{-3}s^{-1}) \times 10^{10}$	b
1	1.66	1.67
2	2.80	1.47
3	1.19	1.85
4	1.00	1.55
5	1.30	2.24

It has been observed that intensities of the lines/continuum radiations are strongly dependent of the abundances and number densities of different species, temperature and spatial extent of emitting species.

Recently the line intensities as intense as of ~ 10^{-2} ergs s^{-1} cm^{-2} sr^{-1} are observed from certain PDRs. In order to find a matching input it is required that FUV radiation incident upon the region should be stronger than the average interstellar radiation field by an order of 10^{3}-10^{4} or even in some cases more. This explains that most of the PDRs are associated with certain O/B stars.

It has been argued by de Jong et.al.(1980) that the representative values of work function for the interstellar grains is 6eV. Further FUV radiation incident upon PDRs is having the energy less than 13.6eV. Thus an average energy of radiation field can be assumed safely as 10eV. Thus energy carried by each photo ejected electron is 4eV, which is deposited into the medium. Further it has been found that photo electron yield y of the dust/grain in the interstellar medium is ~ 0.1. Therefore the efficiency (ε) of FUV radiation converted into the heat is (4/10)x0.1 =0.04. i.e.only 4% of FUV radiation are converted into heat. Furthermore, it can be assumed that efficiency of photo-electron emission depends upon the microscopic parameters such as the photoelectric yields and work

functions of the grains but not on the global parameters such as the gas to dust ratio. The efficiency is insensitive to the FUV albedo and absorption cross-sections of the grains.

Fig.(4.1) shows a more quantitative analysis of the photoelectric mechanism which includes the effect of grain charge. Using the formalism derived by de Jong (1980), one can calculate ε as a function of the parameter

$$\gamma = 2.9 \times 10^{-5} G_o T^{0.5} n_e^{-1} \quad \text{---------- (4.31)}$$

The parmeter γ is a measure of the ratio of the rate at which FUV photon strike grains to the rate at which electrons recombine with grains. Thus $\gamma \ll 1$ implies neutral or negatively charged grains where ε is expected to be high (>0.01), where $\gamma \gg 1$ implies positively charged grains. Fig.(4.1) plots ε against γ. Typically, in photodissociation regions which lie between HII regions and molecular clouds, $G_o \sim 10^4$, $n_e \sim 10$ cm^{-3}, and T ~ 100K, so that $\gamma \approx 0.3$ and $\varepsilon \approx 4 \times 10^{-3}$. Therefore , photoelectric heating is a promising mechanism to explain the extended and luminous OI (63μm) and CII (158μm) emission which requires a little high temperature.

Fig (4.2) and (4.3) shows the contours of calculated gas temperature at the surface of the cloud ,T_s, and maximum gas temperature, T_{max}, as a function of n and G_o. Since the gas heating and cooling rates vary with optical depth into the cloud, the gas temperature is not constant through the

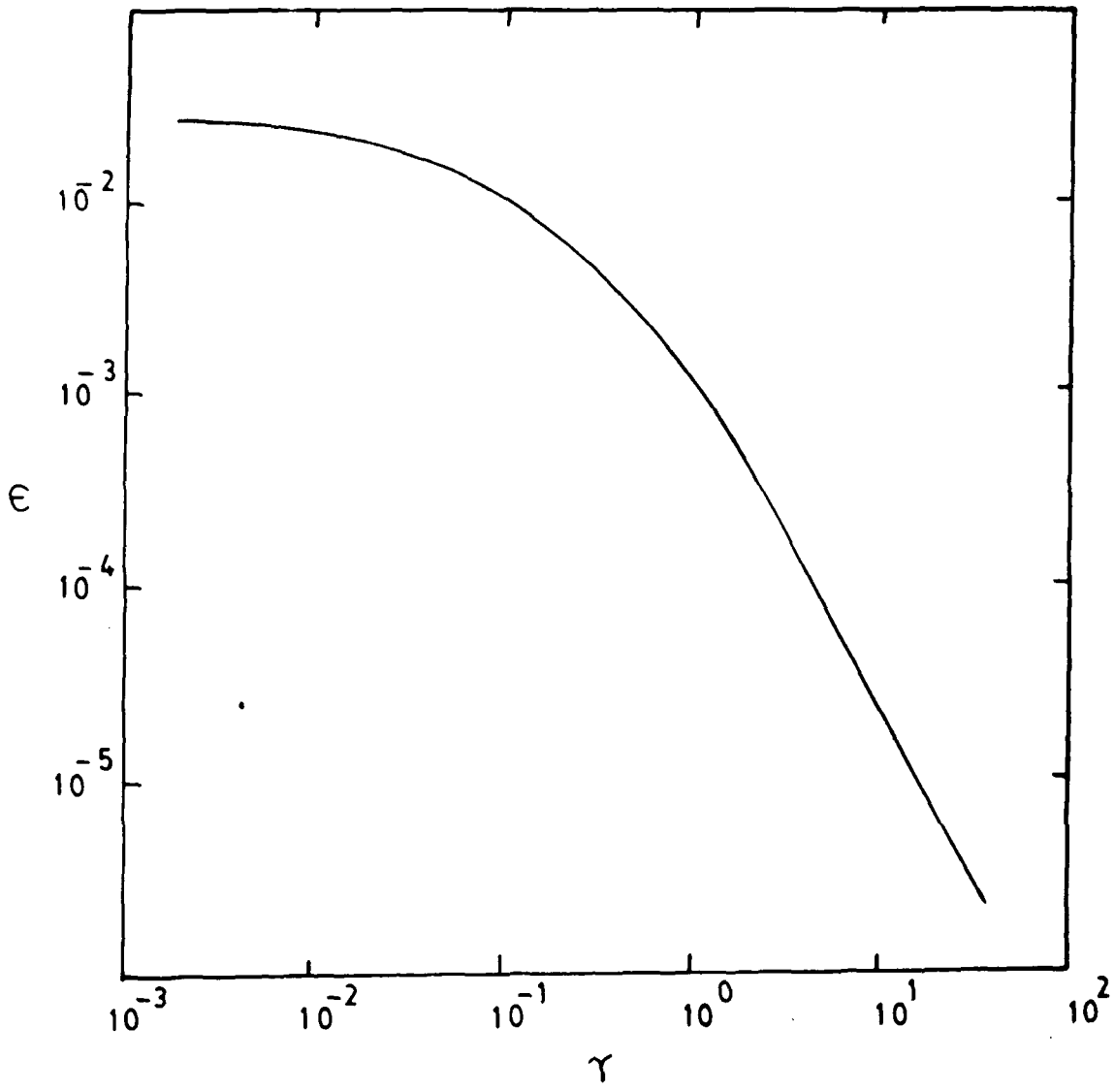

Fig. 4.1 : Photoelectric heating efficiency of the gas as a function of γ .

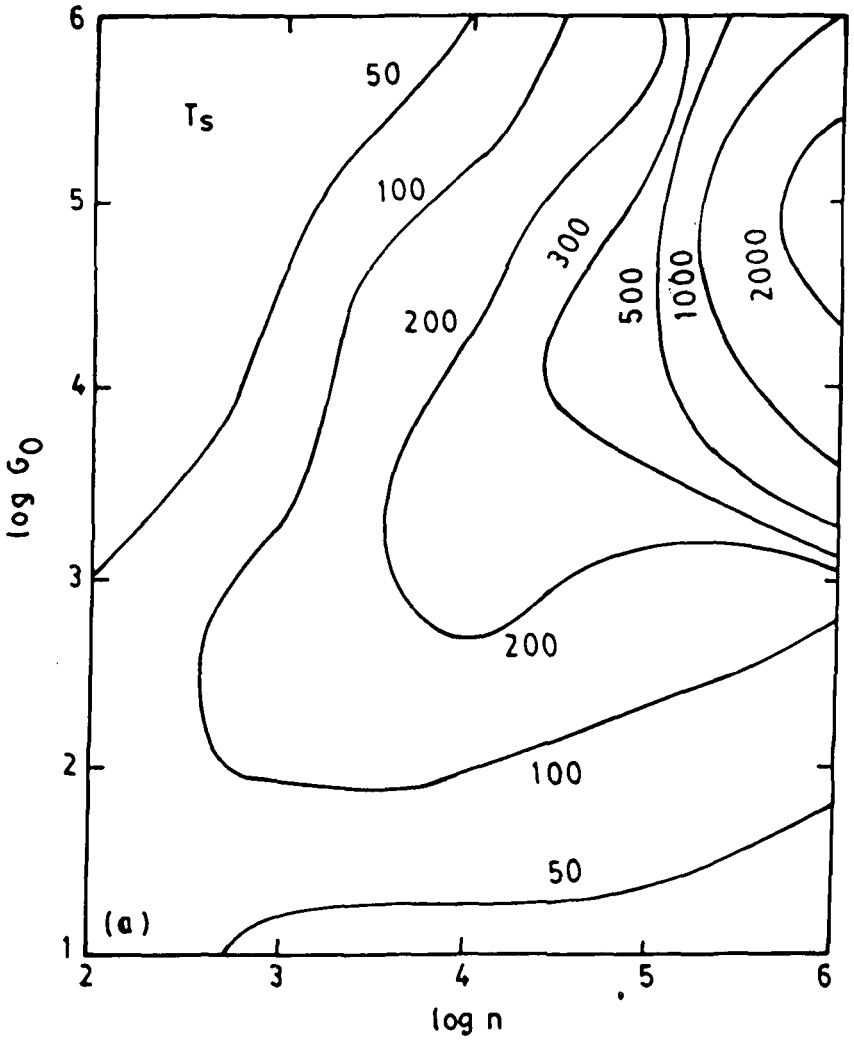

Fig. 4.2 : Contour map of the gas temperature at the surface.

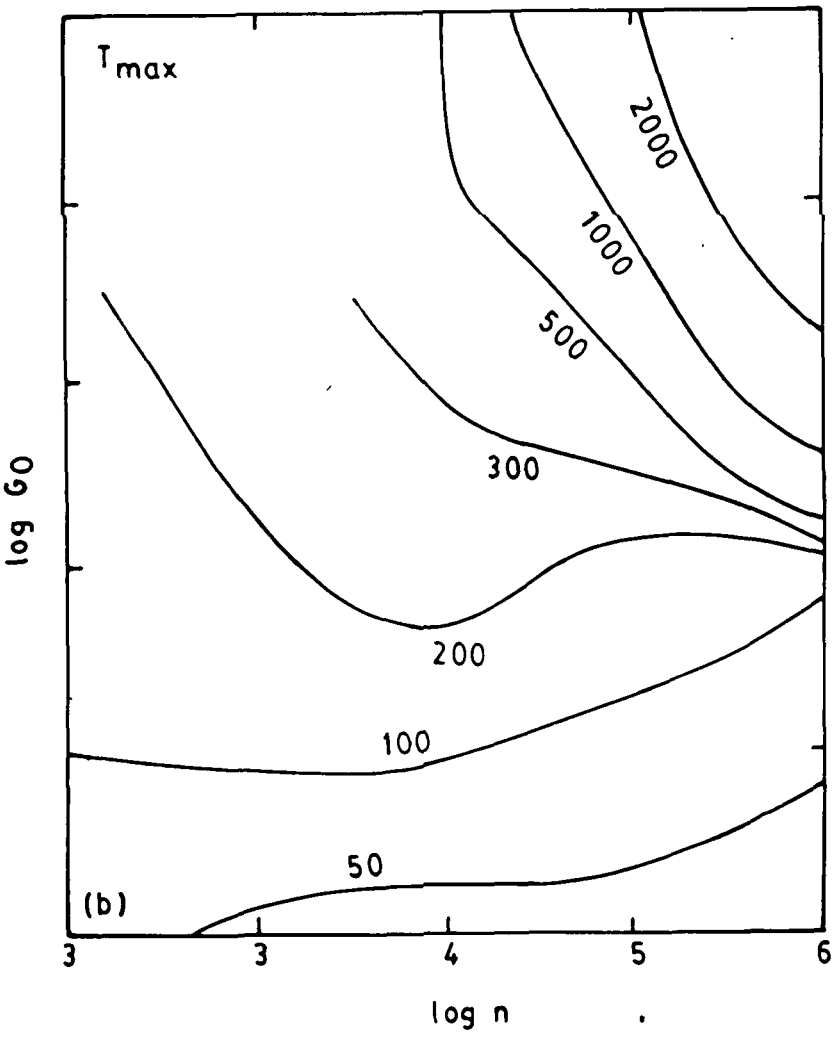

Fig. 4.3 : Contour map of the maximum gas temperature.

photodssociation region. As discussed by THa, photoelectric heating decreases with optical depth into the cloud due to extinction of the incident FUV field. However, the photoelectric heating "efficiency" initially "increases" with optical depth, since dust grains becomes less positively charged. The gas cooling, through infrared fine-structure lines decreases more rapidly than gas heating, since OI (63μm) line becomes optically thick. The resulting temperature profile generally "increases" from the surface temperature, T_s, to a maximum temperature T_{max} ($A_v \sim 1$) and then decreases due to diminishing photoelectric heating. For low G_o no T_{max} will be observed. For cases of low incident FUV field, $G_o \leq 10^3$, and high density, $n \geq 10^3$ cm^{-3}, the grains are quite neutral, the temperature rise is small, and $T_s \approx T_{max}$.

For $G_o \leq 10^3$, the temperature generally increases with G_o but are relatively insensitive to n. This is because the photoelectric heating efficiency becomes nearly constant as grains become neutral or negatively charged. As shown in fig (4.1) this occurs at $G_o T^{0.5} n_e^{-1} \ll 10$. At high FUV fields, $G_o \geq 10^3$, the surface temperature initially increases with G_o but then begins to drop off with increasing FUV flux. In addition, T_s is a strongly increasing function of n. This temperature dependence on n and G_o is a result of high positive grain charge ($G_o T^{0.5} n_e \gg 10$). The photoelectric

heating efficiency rapidly falls as G_o increases. Similarly, as the density increases, the photoelectric heating increases more rapidly with density than the cooling and T_s goes up. At high FUV fields, $G_o \geq 10^3$, and high densities, $n \gg 10^4$ cm^{-3}, the OI (63μm) line dominate the cooling. As densities approach the critical density $n_{cr} \sim 10^5$ cm^{-3}, the OI cooling efficiency drops, and gas temperature rise to greater than 500K.

For clumpy PDRs the behaviour of temperature structure will be almost similar to that of the homogeneous cloud. But the fall of temperature after maxima will not be so rapid because even at this optical depth enough radiation seep into the high density clump through interclump. Due to this reason cooling from oxygen still remain important.

Further for optically thin cloud the surface temperature T_s and maximum temperature T_{max} both are slightly reduced in the finite slab model because of cooling from the surfaces of the slab provided its main coolant is CII. In M17 region it has been found that main coolant near the surface is OI (63μm) line which is optically thick. Therefore, in both the models under discussion escape of radiation is towards observser. Owing to this fact, the temperature structure in the present formalism will be almost same as that in the TH model.

Further deep into the cloud temperature becomes

independent of model assumption because main coolants are lower rotational transitions of CO molecule which are also optically thick and hence permit the radiation to escape through only one face.

THa investigated the effects of independently varying the Doppler width, δv_d, and the C abundance while keeping all other parameters fixed. The gas temperature in the atomic layer should be insensitive to changes in δv_d in the region of parameter space where the optically thin CII line dominates the cooling. When the optically thick OI (63μm) line dominates the cooling, however, T_{max} is sensitive to δv_d. Increasing δv_d by a factor of 5 results in a drop in T_{max} by a factor of ~ 2 in the standard model of THa ($G_o = 10^5$, $n_o = 2.3 \times 10^5$ cm^{-3}). The surface temperature, T_s, is insensitive to changes in δv_d since cooling is optically thin at the cloud surface.

Decreasing the C abundance results in a lower electron abundance and an increased positive grain charge. The photoelectric heating efficiency thus decreases, and the gas temperature drops.

CHAPTER - 5

RESULTS AND DISCUSSIONS

CHAPTER - 5

RESULTS AND DISCUSSIONS

In order to study the physical conditions inside the M17 region a model calculation has been performed for the region using the present formalism. For that purpose density is taken as free parameter while turbulent velocity and flux of the radiation field are taken from the Meixner et. al.(1992). These parameters are derived from the observations. In order to study the effects of the escape of photons from both side of the plane parallel slab a range of densities ($100 \leq N \leq 10,000,000$) are considered but in the figures only upto the maximum value 10,000 are taken because in this range the difference between TH model and the present formalism is substantial.

The temperature of the medium is determined self consistently by solving the energy balance, radiative transfer, and chemistry in the model. Actually, the density and temperature are inter-related in the photoelectric heating mechanism. The temperature of the gas increases with density because the grains are less positively charged and the photoelectric heating mechanism is more efficient (Wolfire et.al. 1990) but increase of flux does not necessarily increase the temperature of the medium because grains become more and more positively charged due to which

photoelectron emission efficiency is decreased. In any case, for the selected parameters, the temperature starts low ~ 50K and ris s to few thousands. This range of parameters covers almost al the range of excitation temperatures of the cooling spe ies considered here (CI, CII, OI, SiII and CO).

The whol range of results can be understood in terms of the three sets of the pairs of parameters of the line emitting region and the line emission itself. The pairs of parameters are following.

(1) Line optical depth and ultraviolet continuum optical depth of dust and gas in the region.

(2) Critical density of the line emission and number density of the line emitting region.

(3) Line excitation temperature and the kinetic temperature of the line emitting region.

The excitation conditions of the cooling lines are given in Table (5.1). It is expected and found that the line intensity will peak at the point in the region where its excitation conditions are optimal.

As mentioned earlier that ultraviolet optical depth is very important factor because it determines penetration of FUV flux inside the region which in turn decides the thermal structure of the region, the spatial extension of the line emitting region, abundance of the medium etc. In order to study the FIR and sub-millimeter line emissions earlier

TABLE - 5.1

Excitation conditions of cooling lines

Line	$\lambda(\mu m)$	N_{cr}	Eexc(K)
CII	158	2.8(3)	92
CI	370	4.7(2)	24
CI	609	2.8(3)	63
OI	63	4.7(5)	228
OI	145	9.5(4)	326
SiII	35	3.4(5)	414
CO (1-0)	2602	1.6(3)	5.5
CO (4-3)	651	6.7(4)	55
CO (8-7)	325	5(5)	200
CO (14-13)	186	3.2(6)	580

The digits in parentheses should be read as powers of 10

attempts were made to calculate the line intensities assuming homogeneous medium. Analysis in terms of a homogeneous model yields an incident UV field of 5.6 x 10^4 Habings and a density of ~ 3 x 10^4 cm^{-3} and a temperature of ~ 300K for atomic gas.

However, various line intensities and spatial distributions are unsatisfactorily reproduced. Indeed, several considerations imply that the M17 PDR is clumpy in nature. For example, the spatial extent of the various FIR fine structure lines and the FIR continuum suggests that the UV field penetrates far deeper into the molecular core, as expected with the homogeneous model. Pronounced evidence for clumpiness in PDRs are the parsec scale lengths of [CII] 158μm emission observed in Orion (Stacey et.al. 1992), M17 SW (Stutzki et.al. 1988), and W_3, NGC 1977, and NGC 2023 (Howe et.al. 1991). Homogeneous PDR with typical densities of 10^4-10^5 have an extent of ~ 0.01 Pc when viewed edge-on. However, the fact that the CII emission extends from ~ 1 Pc in NGC 1977 to around 4 Pc in W_3 and M17 SW (all three regions are viewed edge-on) indicates that the PDR extends quite far into these regions. The spatial distribution of the line emission follows the temperature distribution of the medium, clump or interclump, which ever contributes most of the emission at that location. the temperature distribution reflects the UV penetration, into the region, the crux of the

difference between the homogeneous and clumpy models.

In addition to the gas temperature profile, the chemistry of the gas component influences the edge-on spatial profile. In a homogeneous PDR, the chemical composition of the gas changes as a function of depth into the region: HI become H_2 and CII becomes CI and CO. In a clumpy PDR, these transitions occur at different depths into the region for each component. Each clump is an "island" PDR with the transitions occuring in each clump, thereby providing all chemical states at each point in the UV illuminated region.

The line intensities of different cooling agents are plotted in the figures (5.1 - 5.2) for different number densities of hydrogen upto a maximum of 10,000 and compared with that of TH model. The calculation with large densities are not shown here because the line intensities calculated by TH model and the present formalism merge together. Further the densities considered here are representative of the interclump medium. The line optical depth parameter divides the PDR cooling lines into two groups: (a) optically thin lines [CII (158μm), CI (609,370μm), OI (145μm), SiII (35μm) and high rotational transitions of CO] and (b) optically thick lines [OI (63μm) and low rotational transitions of CO].

First we cosider the optically thin lines with low excitation conditions [CI (370 and 609μm)]. These lines are plotted in fig (5.1). It is quite clear from the figure that

present calculation differ with that of TH model calculation When the density is sufficiently low the radiation term dominates and lines are influenced very much. But as the density increases the line intensities calculated by both the formalism are approaching each other and finally merge together. One important factor worth mentioning is the variation in the line intensity that also depends upon the UV radiation which governs the temperature. If the temperature is sufficiently low then the difference between both the formalism will be maintained even for a larger densities.

For optically thin and high excitation condition lines the difference between the two different formalisms under discussion is found to be almost an order of magnitude at low density [fig (5.4) and (5.5)] where SiII and high rotational transitions of CO are compared. It is also found that SiII line and high rotational transitions of CO differ from TH values even at sufficiently high density because of their high excitation conditions. Therefore, under such conditions TH model is not appropriate to calculate the line intensities. Fig. (5.6) is for homogeneous cloud with a density of 10,000 and for flux of 5.6×10^4 Habing. In this case too it can be seen that even at such high densities the high rotational transition intensities differ by an order of magnitude with that of TH model. The difference for 14-13 transition is narrowed down for density greater than

10,000.000. But whole scenario will be changed if temperature or UV flux is varied. These lines are very sensitive to temperature.

CII (158μm) line is moderate in both the sense (optical depth around unity and excitation conditions are also neither low nor high). The intensity for the line is plotted in the fig. (5.1). For low density the difference between the two formalism under discussion is obvious. But at density around 100,000 or greater the difference is not found to be substantial. The difference between the models under discussion may vary with the variation of UV radiation.

From the figures (5.3), (5.5) and (5.6) where optically thick lines are plotted, it is clear that when lines are optically thick no substantial difference is found. In the optically thick lines the radiation can escape only from one side of the cloud. Therefore, the cloud may be assumed behaving as semi-infinite as assumed by de Jong et.al. (1980) Further if we put ($T_\nu \to \infty$) in the equation (2.30) this will be reduced to the exactly same form as used by TH. Therefore, for optically thick lines TH model can be employed safely. If we analyse the figures (5.3), (5.5)and (5.6) even in terms of optically thick case then we may notice a difference between OI (63μm) and low rotational transitions of CO. For the low rotational transitions starting from the low density both the approaches are yielding same results fig. (5.5) and (5.6).

But in case of OI (63μm) [fig. (5.3)] at low density a little departure exist even if flux and other parameters of the cloud are changed.

In figures (5.7) and (5.8) calculated line intensities are compared with that of the corresponding observed values. The clump and interclump densities are taken as 6×10^{5} cm^{-3} and 4×10^{3} cm^{-3} while corresponding turbulent velocities are 1.5 Km/s and 7.8 Km/s respectively. The UV flux is 5.6×10^{4} units of Habing. From the figures it is observed that the line intensities for the fine structure transitions of atoms and ions from the interclump are smaller than the corresponding transitions from the clumps figure (5.7). It is also evident from the same figure that the line intensities for fine strucure transitions from the clump agree fairly well with that of the corresponding line observations except OI (63μm). The interclump intensity of the OI (63μm) line is low enough than the clump but it comes out to be close to the observed value. The contribution of the interclump is negligible except CII whereas the interclump intensity of CII is comparable to the observations. In figure (5.8) both the calculated and observed line intensities are plotted for the rotational transitions from the clump and interclump upto the J = 14. In case of CO molecule too, for the given range of parameters of the cloud, the line intensities from the clump are fairly in good agreement with that of the observations.

The contribution to the rotational line intensities from the interclump are negligibly small except the first level transitions of CO.

As mentioned earlier that calculated line intensity of OI (63μm) is higher by an order of magnitude as compared to that of observations in case of the clump but it is slightly lower in the case of interclump. If we consider the absorption of 63μm line radiations from the clump inside the interclump then its intensity will be reduced further and may come close to the observed value. It can be concluded that observed OI lines are from the clump because these are not found in the extended region Meixner et.al. (1992). Further OI (63μm) line is found to be peaked with the CII and SiII lines. The contribution to the line intensity of silicon from the extended region is minimal because of high excitation conditions. Therefore, these are from the dense clumps. So far as line intensities of CII are concerned the calculations show that clump and interclump line intensities are comparable. Therefore these lines may be found in the extended region. It has been observed by Stutzki et.al (1988) that two peaks of CII are almost 1 Pc. apart. This much extension may not be explained even from the clumpy structure of M17 region. As expected CI lines will be explained even from the interface because carbon will be in the ionized form due to large UV flux. The same thing is observed and

concluded by Meixner et.al. (1992). Further calculation shows that contribution to the line intensity from clump and interclump both are comparable. Therefore, first transition of CO may be observed from the extended region. Meixner et.al. (1992) has shown that CO (7-6) and CO (2-1) peak together. This also shows that these radiations are from the clumps. Further spatial extended observations of first transitions of CO will give more insight to the clumpy structure of M17 region.

Conclusions:

The conclusions drawn from the present study can be summarised as follows,

(i) The clumpy structure of the cloud allows the FUV radiation to penetrate more and more deep into the region as compared to the homogeneous medium. This explains the observed large spatial extent of CII in M17 region.

(ii) Two distinct features of CII and CI lines observed in M17 region also explain the clump surrounded by the interclump. Further radial velocities of clump and interclump are also different.

(iii) The observed and calculated values are found to be in close agreement over a wide range of fine structure emission and rotational transitions. This also indicate the clumpiness in the medium. The densities for clump and interclump medium of M17 are estimated to be around 6×10^5 and 4×10^3 cm^{-3}

respectively.

(iv) It is also found that most of the lines are originating from the clumps. But extended line emissions are possible in the case of CII (158μm), CI (370 & 609μm), OI (63μm) and CO (1-0) emission. For CII and CI it is observed.

(v) The calculated line intensity may come close to the observed value if absorption by interclump is also considered.

(vi) Most of the observed lines are optically thin except OI (63μm) and low rotational transitions of CO molecules. For optically thin lines TH model overestimate the line intensities because all of the radiations are allowed to escape only towards the observer. Therefore, for optically thin lines semi-infinite slab assumption of de Jong et.al. (1980) is not tenable. However for optically thick lines both the assumptions (i.e. semi-infinite and finite slab) converge to the same value. Therefore, TH model can be employed safely for optically thick lines.

(vii) The optically thin line intensities calculated using the finite slab assumption differ from that of the TH model. The difference in the intensities is dependent of the critical density of the line. For CII line emission, line intensity calculated using the present formalism is almost half of that of TH model. But for higher rotational transitions of CO molecule they differ by an order of

magnitude or more.

(viii) At higher densities far greater than the critical density radiative processes have no role to play, therefore, TH model agrees fairly well with the present formalism. For optically thick lines too TH model can be employed safely.

(ix) The temperature structure in both the formalism as discussed above is almost same and is insensitive to the model assumption. This is due to fact that in M17 region most of the cooling at the surface or near the interface of CII/CI/CO is mainly due to the OI (63μm) line emission. This line is optically thick. As it has been already discussed that for optically thick lines both the formalism converge to the same point. Therefore, temperature structure will remain same. In the interior of the cloud most of the cooling is due to low rotational transitions of CO which are also optically thick. Thus temperature structure is insensitive to the model assumption.

(x) The strength of FIR and sub-millimeter lines is quite sensitive to the FUV flux and also to the assumption as discussed earlier.

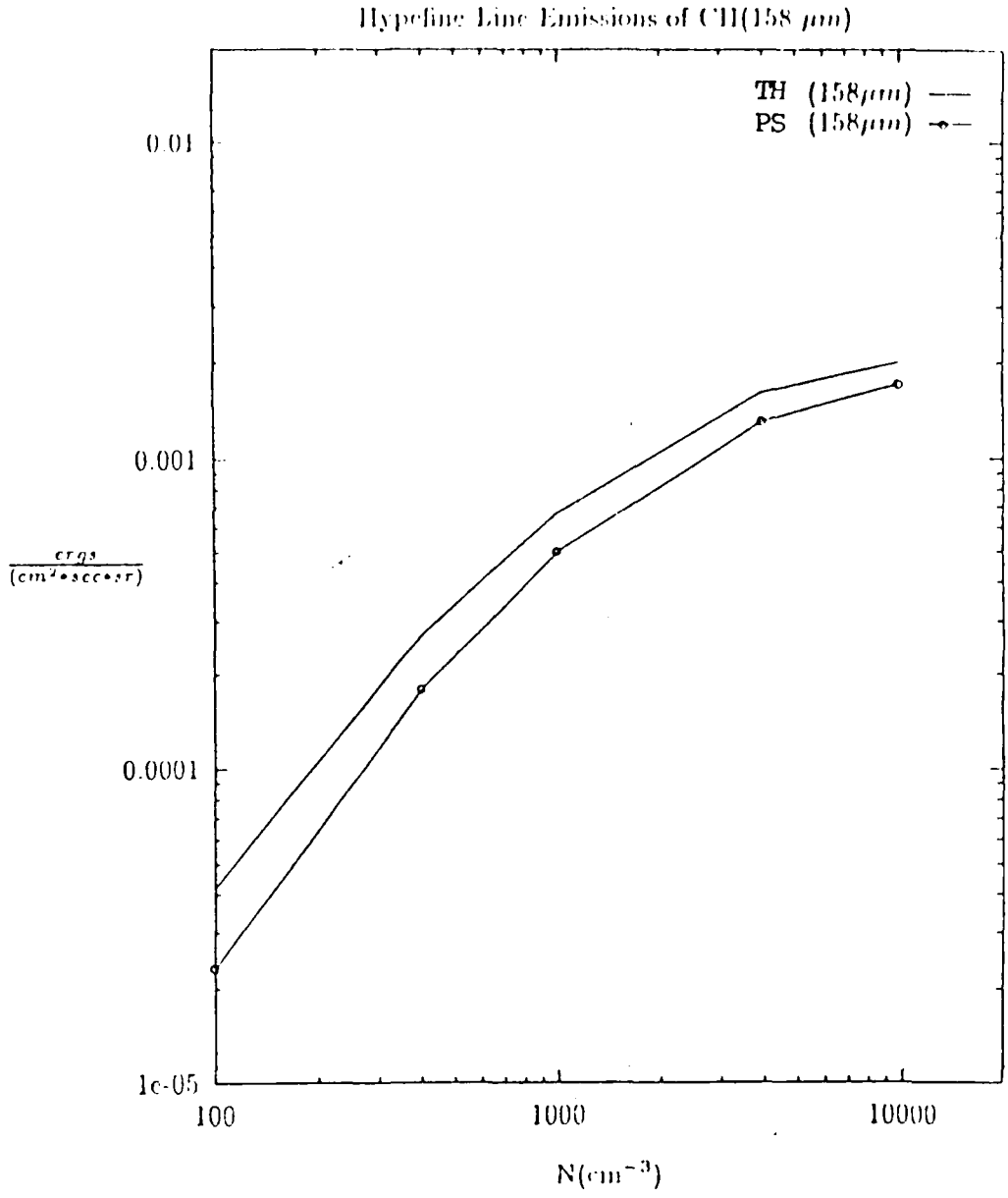

Fig. 5.1

CII(158 μm) line intensity of 'interclump' vs interclump density (N) for clump density of 5.6×10^4

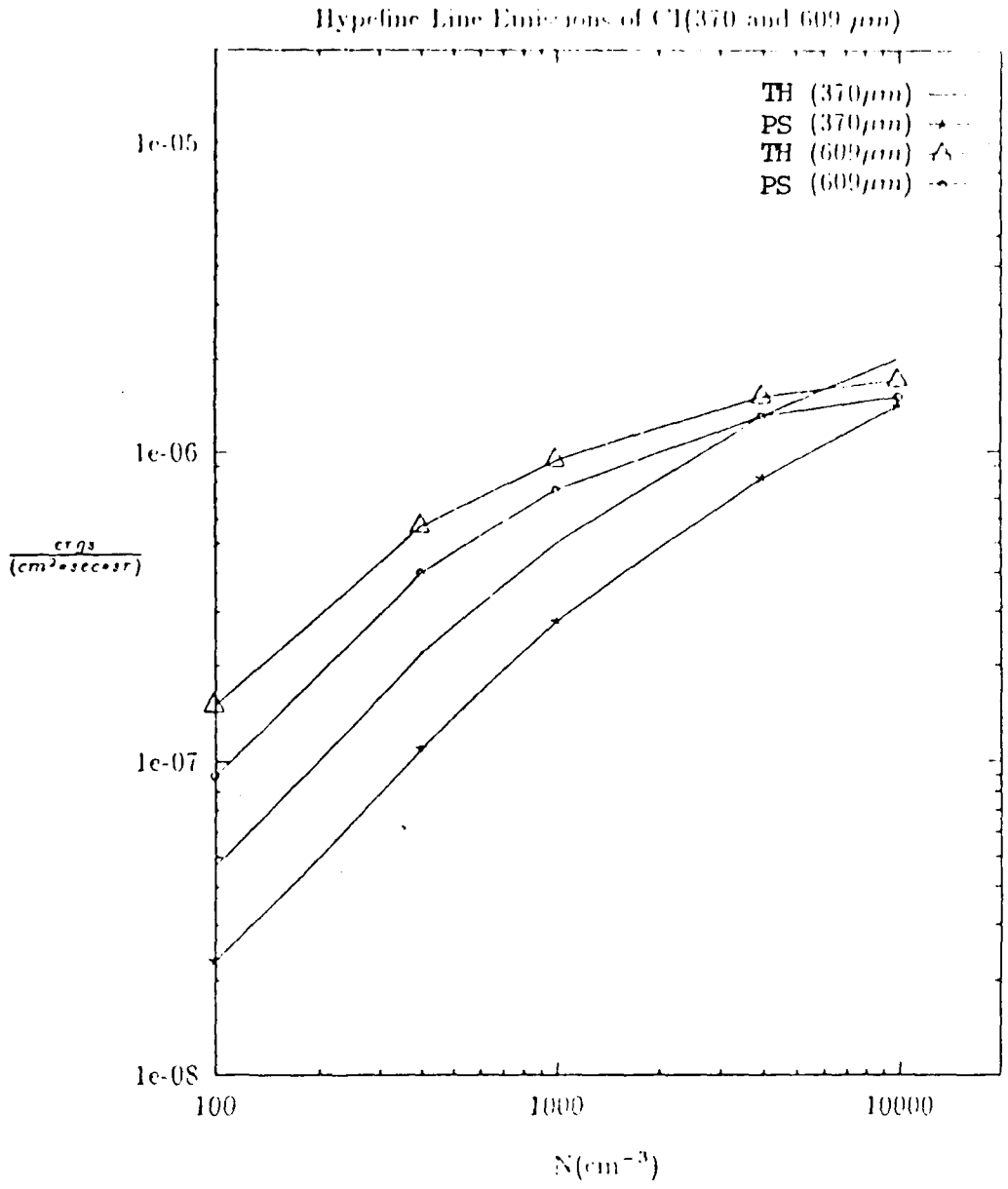

Fig. 5.2

CI(370 and 609 μm) line intensity of 'interclump' vs interclump density (N) for clump density of 5.6×10^4

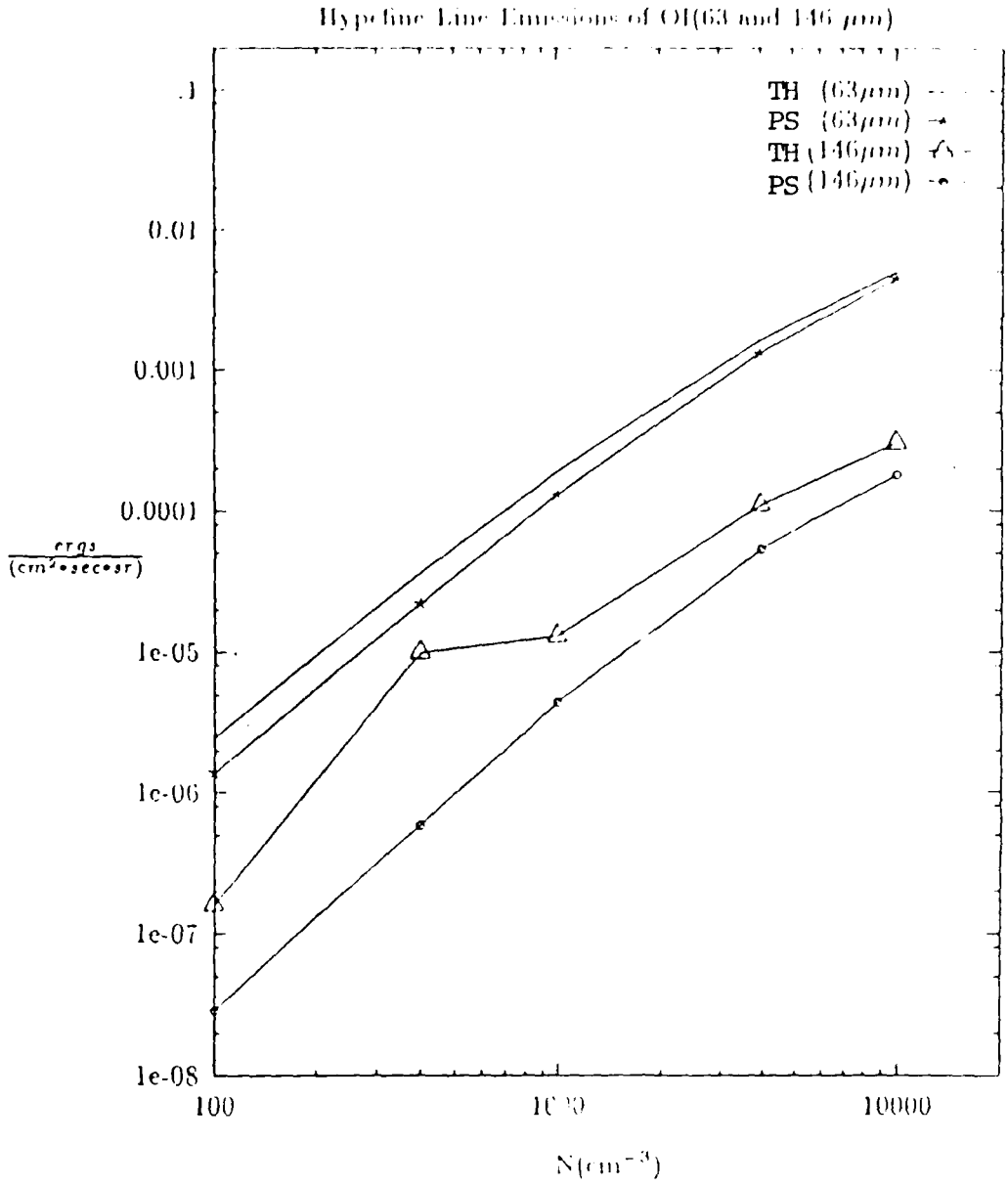

Fig. 5.3

OI(63 and 146 μm) line intensity of 'interclump' vs interclump density (N) for clump density of 5.6×10^{4}

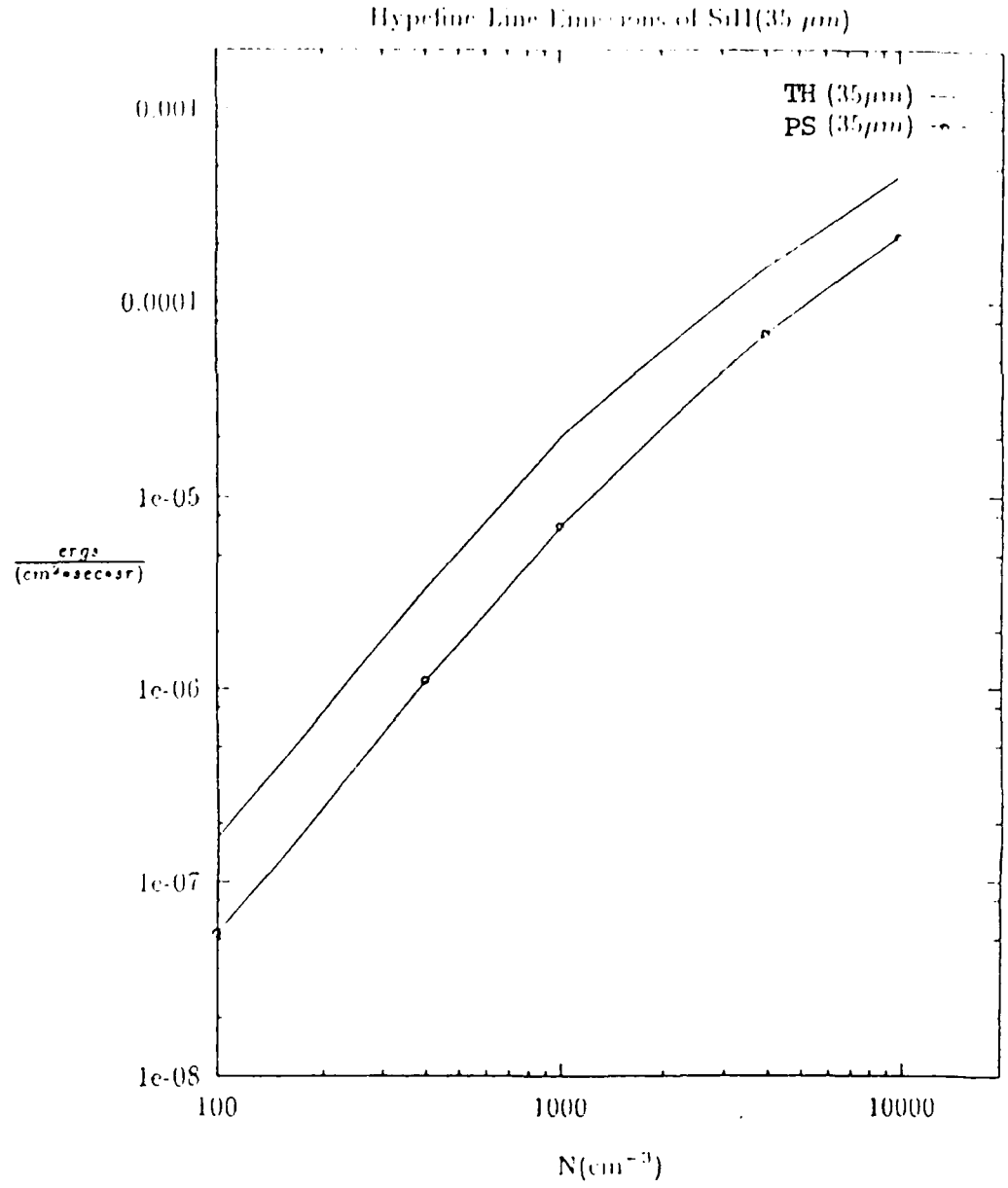

Fig. 5.4

SiII(35 μm) line intensity of 'interclump' vs interclump density (N) for clump density of 5.6×10^4

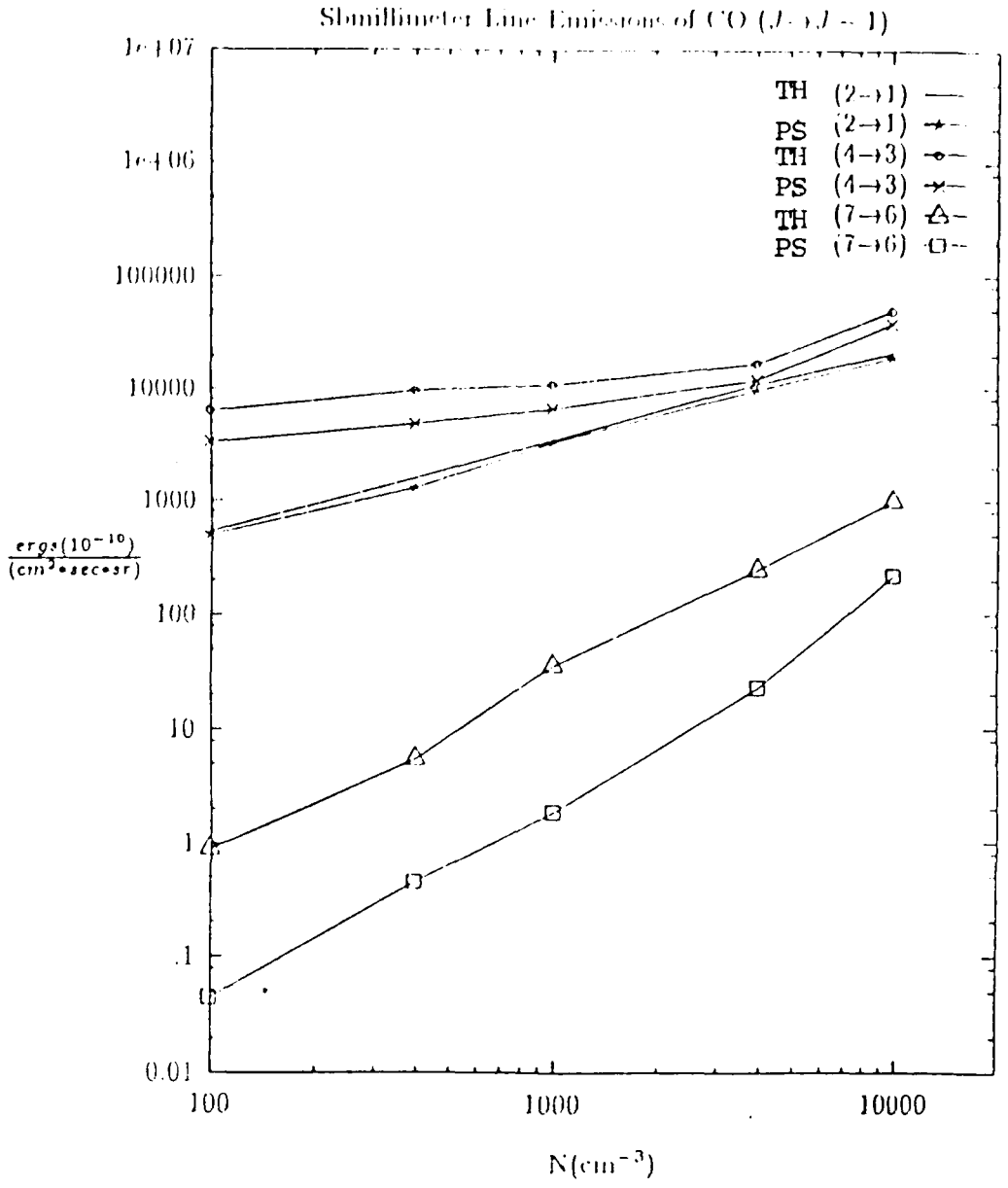

Fig. 5.5

Line intensity of CO(2→ 1, 4→ 3, 7→ 6) transitions.Intensity vs interclump density fo clump density of 5.6×10^4

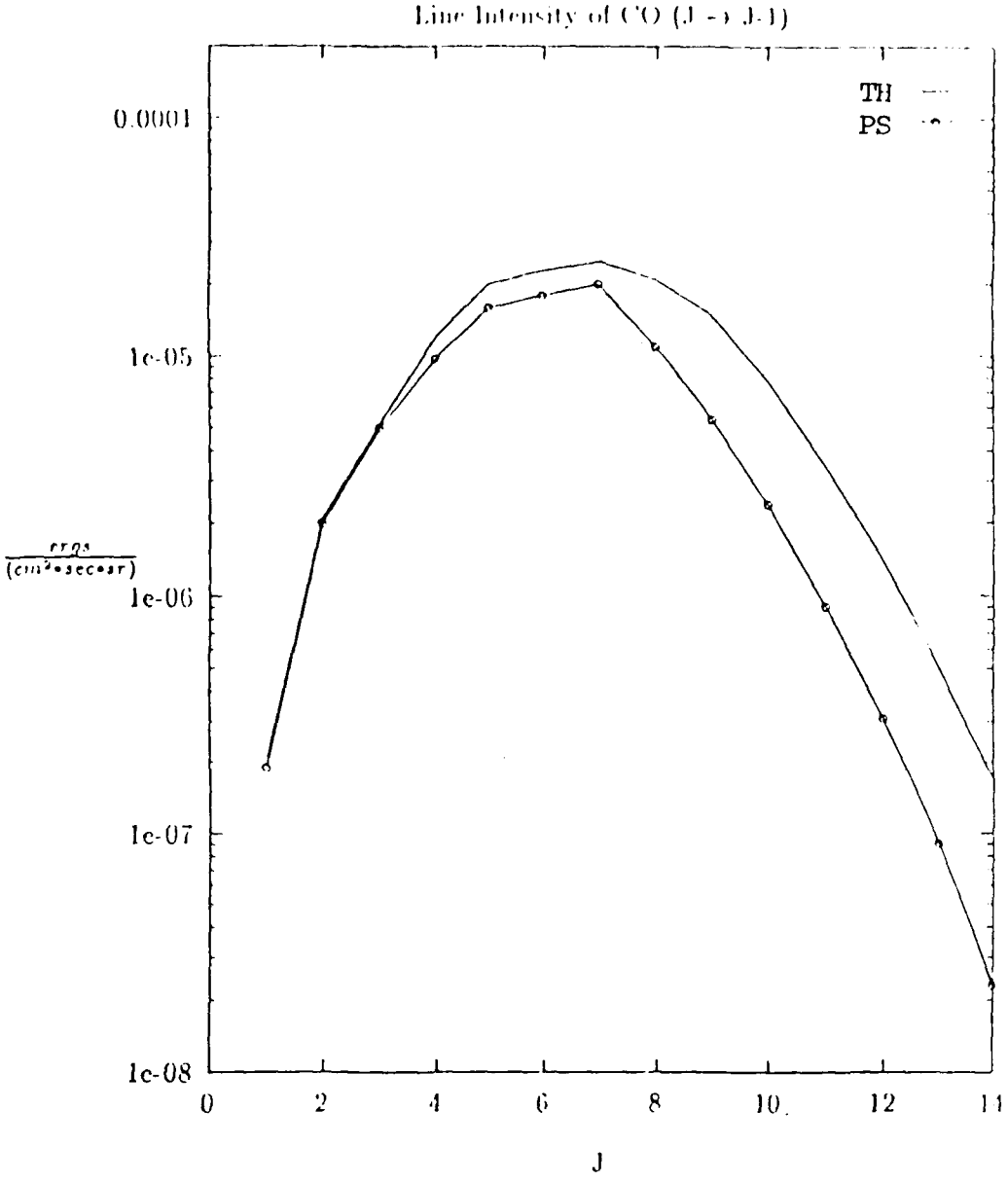

Fig. 5.6
Line Intensity of Different J (transitions) vs Level J for CO molecule in Homogeneous PDR of density 10^5 cm^{-3} and G0 = 5.6×10^4

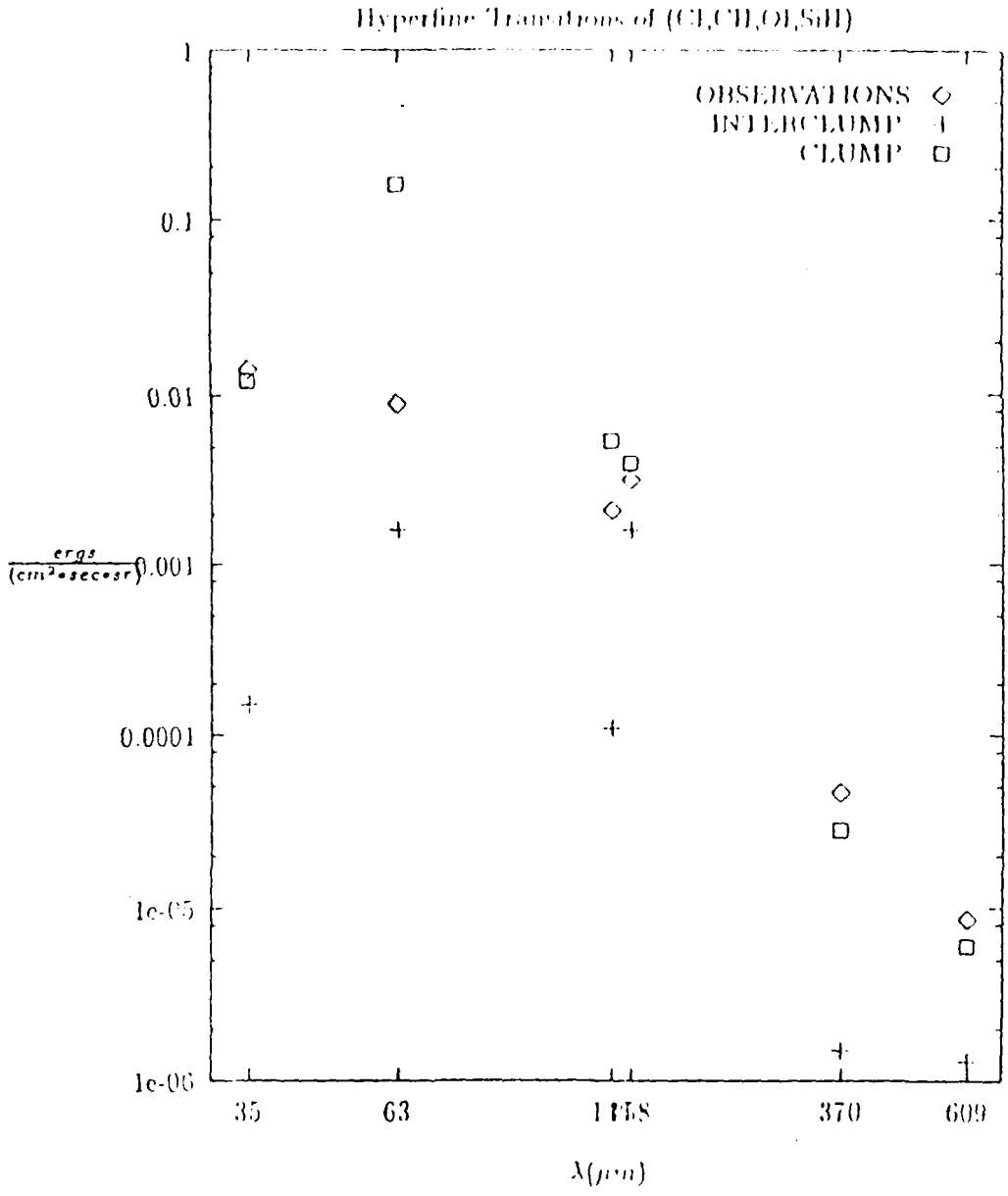

Fig. 5.7

Line intensities of FIR fine structure line emissions of CII(158μm),CI(370 and 609 μm), OI(63 and 146 μm), SiII (35 μm) in the 'interclump' and 'clump' medium for their densities of 4×10^3 and 6×10^5 and $G0 = 5.6\times10^4$

Observed values(References): CII(158μm) Stutzki et al 1988; CI(609 μm) Keene et al 1985; CI(370 μm) Zmuidzinas et al 1986; OI (63 μm) Meixner et al 1992; OI(146 μm) Meixner et al; SiII(35 μm) Meixner et al

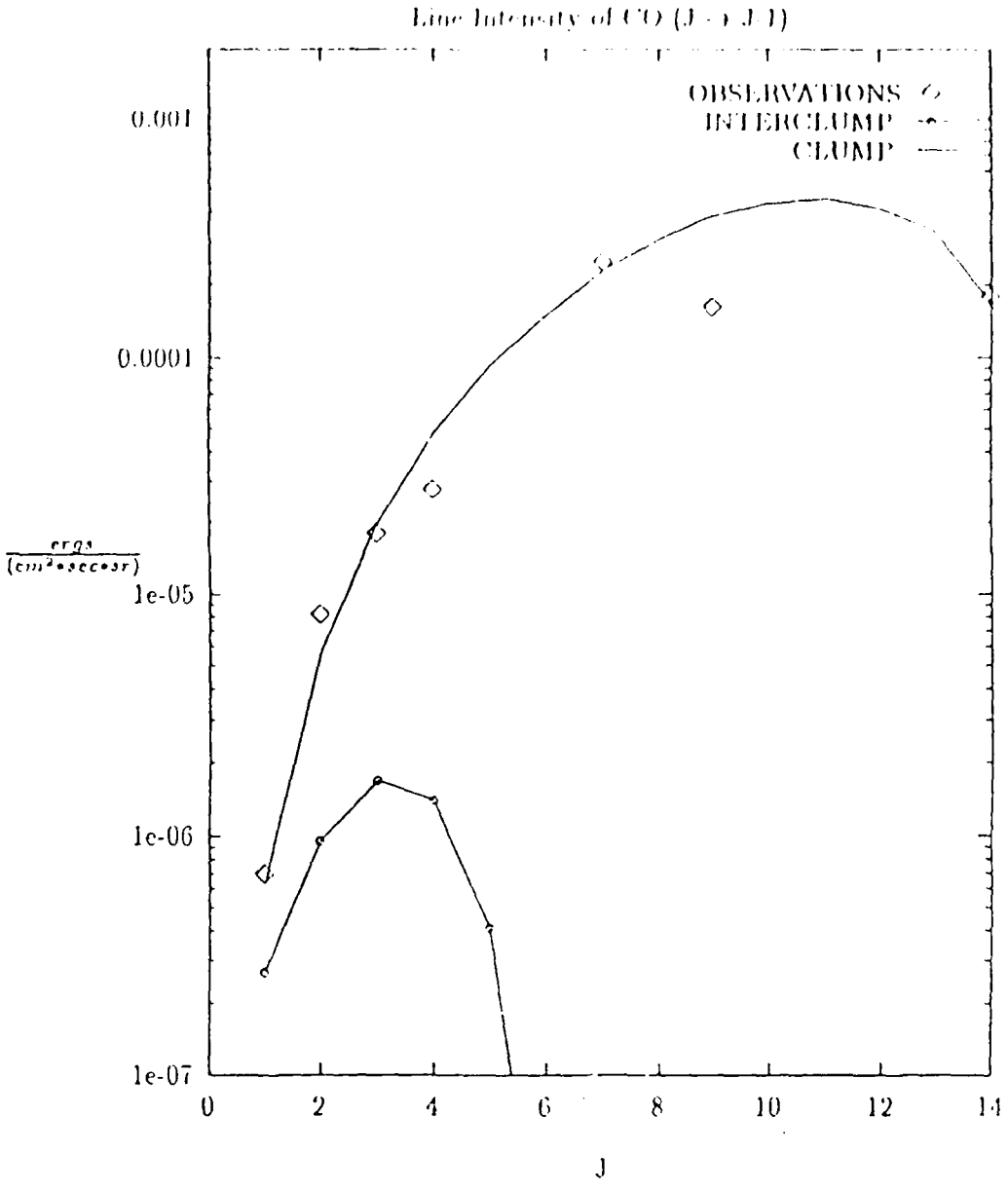

Fig. 5.8

Line Intensities of transitions (J→J − 1) of CO molecule in the 'interclump' and 'clump' medium for their densities of 4×10^3 *and* 6×10^5 *and G0 = 5.6×10⁴*

Observed values:(References) (1→0) *Thronson et al 1988;* (2→1) *Lada 1991;* (3→2) *Rainey et al 1987;* (4→3) *Schulz and Krugel 1987;* (7→6) *Stutzki et al 1988 ;* (9→8) *Boreiko and Betz 1991;* (14→13) *Harris et al 1987*

CHAPTER - 6

BIBLIOGRAPHY

CHAPTER - 6

BIBLIOGRAPHY

Averett, E. H., and Hummer, D. G., 1965, MNRAS, 130, 295

Bennet, C. L., Fixson, P. J., Hinshaw, G.W., Mather, J. C., Moseley, S. H., Wright, E. L., Eplee jr, R. E., Gales, J., Hawagana, T., Issacman, R. B., Shafer, R. A., and Turpie, K., 1994 Ap. J., (Submitted)

Black, J. H., and Dalgarno, A., 1977, Ap. J., suppl. 34, 305

Boisse, P., 1990, A & A, 228, 483

Boreiko, R. T., and Betz, A. L., 1991, Ap. J., 369, 382

Castets, A., Duvert, G., Durtey, A.,Balley, J., Langer, W. D. and Wilson, R. W., 1990, A & A, 234, 469

Compaan, A., Langer, W. D., Eden, D., and Swinney, H. L. 1973 Ap. J., 185, L105

Crutcher, R. M., and Watson, W. D., 1985, in *Molecular Astrophsics*, eds. G. H. F. Dierckson, W. F. Huebner, and P. W. Langhoff, NATO ASI series 157, Riedel, Dordrecht, P. 255

Dalgarno, A., and Black, J. H., 1976, Rep. Prog. phys. 39,573

Dalgarno, A., 1976a, in *Frontiers of astrophysics*, ed. E. H. Averett, Harvard university, P. 352

Dalgarno, A., 1988, Astro. Lett. and Communications, 26, 153

de Jong, T., Chu, S. I., and Dalgarno, A., 1975, 199, 69

de Jong, T., 1977, A & A, 56, 137

1980, Highlights Astr., 5, 301

de Jong, T., Dalgarno, A., and Boland, W., 1980, A & A, 91,68

Garola, H., and Sofia, S., 1975, Ap. J., 196, 473

Glassgold, A. E., and Langer, W. D., 1973, Ap. J. 178 L147

Goldreich, P., and Kwan, J., 1974, Ap. J. 176, 597

Goldsmith, P. F., 1972, Ap. J., 176, 597

Green, S. and Thaddeus, P., 1976, Ap. J., 205, 766

Habing, H. J., 1968, Bull. Astr. Inst. Netherlands, 19, 421

Harris, A. I., Stutzki, J., Genzel, R., Lugten, J. B., Stacey, G. J., and Jaffe, D. T., 1987, Ap. J., 322, L49

Hollenbach, D. J., and Mc Kee, C. F., 1979 Ap. J.suppl, 41, 555

Hollenbach, D. J., Takahashi, T., and Tielens, A. G. G. M., 1991, Ap. J., 377, 192

Howe, J. E., Jaffe, D. T., Genzel, R., Harris, A. I., Stcey, G. J., and stutzki, J., 1991, Ap. J., 353, 193

J. H. Black, 1987, in *Interstellar processes*, eds. D. J. Hollenbach, and H. A. Thronson Jr., Riedel, dordrecht, p. 731

Keene, J., Blake, G. A., Phillips, T. G., Huggins, P. J., and Beichman, C. A., 1985, Ap. J., 299, 967

Miexner, M., Hass, M. R., Tielens, A. G. G. M., Erickson, E. F., and Werner, M., 1992, Ap. J., 390, 499

Miexner, M., and Tielens, A. G. G. M., 1993, Ap. J., 405, 216

Mihals, D., 1970, Freeman, San Francisco

Rainey, et.al., 1987, A & A, 171, 252

Robert, C., and Pagani, L., A & A, 1993, 271, 282

Sciama, D. W., 1993, Ap. J., 409, L25

Scoville, N. Z., and Solomon, P. M., 1974, Ap. J., 187, L67

Schulz, A., and Krugel, E., 1987, A & A, 171, 252

Stacey, G. j., Jaffe, D. T., Geis, N., Genzel, R., Harris, A. I., Poglitsch, Stutzki, J., and Townes, C. H., 1993, Ap. J., 404, 219

Stutzki, J., Stacey, G. J., Genzel, R., Harris, A. I., Jaffe, D. T., and Lugten, J. B., 1988, Ap. J., 332, 379

Thronson, H. A.jr, and Lada, C. J., 1983, Ap. J., 269, 175

Tielens, A. G. G. M., and Hollenbach, D.,1985a,(THa), Ap. J., 291, 722, 1985b,(Thb), Ap. J., 291, 747

Turber, J. A., and Goldsmith, P. F., 1990, Ap.J., 356, L63

Van Dishoeck, E. F., and Black, J.H., 1988a, in *Rate Coefficients in Astrochemistry*, eds. T. J. Miller, and D. A. Williams, Kulwer, Dordrecht, P. 209

Van Dishoeck, E. F., in *Molecular Astrophysics* ed. T. W. Hatquist, Cambridge University, P. 55

Watson, W. D., 1972, Ap. J., 176, 103

Watson, W. D., 1978, Ann. Rev. Astr. Astrophys. 16, 585

Werner, M. W., 1970, Ap. Letters, 6, 81

Wolfire, M. G., Hollenbach, D., and Tielens, A. G. G. M., 1989, Ap. J., 344, 770

Wolfire, M. G., Tielens, A. G. G. M., and Hollenbach, D.,

1990, Ap. J., 358, 116

Zmuidzinas, J., Betz, A. L., and Goldhaber, D. M. 1986 Ap. J. 307, L75